Clathrin-dependent mechanisms modulate the subcellular distribution of class C Vps/HOPS tether subunits in polarized and nonpolarized cells

Stephanie A. Zlatic[a,b], Karine Tornieri[b], Steven W. L'Hernault[a,c,d], and Victor Faundez[a,b,d]
[a]Graduate Program in Biochemistry, Cell, and Developmental Biology, [b]Department of Cell Biology, [c]Biology Department, and [d]Center for Neurodegenerative Diseases, Emory University, Atlanta, GA 30322

ABSTRACT **Coats define the composition of carriers budding from organelles. In addition, coats interact with membrane tethers required for vesicular fusion. The yeast AP-3 (Adaptor Protein Complex 3) coat and the class C Vps/HOPS (HOmotypic fusion and Protein Sorting) tether follow this model as their interaction occurs at the carrier fusion step. Here we show that mammalian Vps class C/HOPS subunits and clathrin interact and that acute perturbation of clathrin function disrupts the endosomal distribution of Vps class C/HOPS tethers in HEK293T and polarized neuronal cells. Vps class C/HOPS subunits and clathrin exist in complex with either AP-3 or hepatocyte growth factor receptor substrate (Hrs). Moreover, Vps class C/HOPS proteins cofractionate with clathrin-coated vesicles, which are devoid of Hrs. Expression of FK506 binding protein (FKBP)–clathrin light chain chimeras, to inhibit clathrin membrane association dynamics, increased Vps class C/HOPS subunit content in rab5 endosomal compartments. Additionally, Vps class C/HOPS subunits were concentrated at tips of neuronal processes, and their delivery was impaired by expression of FKBP–clathrin chimeras and AP20187 incubation. These data support a model in which Vps class C/HOPS subunits incorporate into clathrin-coated endosomal domains and carriers in mammalian cells. We propose that vesicular (AP-3) and nonvesicular (Hrs) clathrin mechanisms segregate class C Vps/HOPS tethers to organelles and domains of mammalian cells bearing complex architectures.**

Monitoring Editor
Keith E. Mostov
University of California, San Francisco

Received: Oct 5, 2010
Revised: Mar 2, 2011
Accepted: Mar 8, 2011

INTRODUCTION

Membranous organelles maintain their steady-state structural and functional identity despite the continuous flow of protein and lipids through them. Flow is dictated by departing carriers budding off organelles and incoming vesicles fusing with their targets. Thus fidelity in vesicle budding and fusion is central to generating and maintaining organelle identity. Coats and adaptors specify vesicle-budding events by selecting cargoes loaded into vesicle carriers. In contrast, Soluble NSF Attachment Protein REceptors (SNAREs), rabs, and tethers determine vesicle fusion fidelity (Bonifacino and Glick, 2004). Vesicular and nonvesicular mechanisms regulate flow of macromolecules between endosomes in mammals. Flow between compartments along the endocytic pathway occurs by vesicle-mediated mechanisms (Stoorvogel *et al.*, 1996; Peden *et al.*, 2004), and the processes of tubule-mediated transfer of cargoes (Delevoye *et al.*, 2009), kiss-and-run (Bright *et al.*, 2005), and endosome maturation (Stoorvogel *et al.*, 1991; Rink *et al.*, 2005; Poteryaev *et al.*, 2010). Here we show that the coat clathrin interacts with endosomal tethers involved in endosome maturation and fusion (class C Vps/HOPS subunits) by means of vesicular (clathrin and the clathrin adaptor AP-3 [Adaptor Protein Complex 3]) and nonvesicular mechanisms (clathrin and hepatocyte growth factor receptor substrate, Hrs).

This article was published online ahead of print in MBoC in Press (http://www.molbiolcell.org/cgi/doi/10.1091/mbc.E10-10-0799) on March 16, 2011.

Address correspondence to: Victor Faundez (faundez@cellbio.emory.edu).

Abbreviations used: AP-3, Adaptor Protein Complex 3; CHC, clathrin heavy chain; CLC, clathrin light chain; DSP, dithiobissuccinimidyl propionate; FBS, fetal bovine serum; FKBP, FK506 binding protein; GFP, green fluorescent protein; HA, hemagglutinin; HOPS, HOmotypic fusion and Protein Sorting; HPS, Hermansky Pudlak Syndrome; Hrs, hepatocyte growth factor receptor substrate; Ig, immunoglobulin; mAb, monoclonal antibody; PBS, phosphate-buffered saline; SNARE, Soluble NSF Attachment Protein Receptor; VAMP7, vesicle-associated membrane protein 7.

Mammalian endosomes possess clathrin domains in the form of budding profiles that contain AP-1/AP-3 clathrin adaptors (Stoorvogel *et al.*, 1996; Peden *et al.*, 2004; Theos *et al.*, 2005) or as flat lattices defined by the presence of Hrs (Raiborg *et al.*, 2002, 2006). Of these coats, buds containing AP-3 and clathrin mature into vesicles that transport their contents between early endosomes and late endosomal/lysosomal compartments (Di Pietro and Dell'Angelica, 2005; Dell'Angelica, 2009). In contrast, *Saccharomyces cerevisiae* generates AP-3 vesicles at the Golgi complex destined for the lysosomal equivalent, the vacuole (Odorizzi *et al.*, 1998). This process is independent of clathrin in yeast (Seeger and Payne, 1992; Anand *et al.*, 2009). Mutation of the human clathrin adaptor AP-3 causes Hermansky Pudlak Syndrome (HPS), in which lysosome-related organelles such as melanosomes, dense-platelet granules, and lamellar bodies are defective. HPS patients exhibit pigment dilution, bleeding diathesis, and pulmonary fibrosis, and this pathology is directly attributable to defects in vesicular biogenesis (Di Pietro and Dell'Angelica, 2005; Dell'Angelica, 2009). HPS phenotypes are triggered in mice when any one of 15 genes is defective. These 15 gene products assemble into protein complexes: AP-3, BLOC-1 to BLOC-3 (biogenesis of lysosome-related organelles complex), and tethering complexes constituted by class C Vps subunits (Li *et al.*, 2004). Vps33a mutant mice possess a phenotype similar to other HPS mutants, which might be explained by interactions of Vps33a with other HPS complexes (Suzuki *et al.*, 2003). Whether these genetic similarities underlie associations of Vps33a with HPS complexes, such as AP-3, into common complexes is presently unknown. This hypothesis is supported, however, by genetic and biochemical interactions between yeast class C Vps proteins and AP-3 (Anand *et al.*, 2009; Angers and Merz, 2009; Salazar *et al.*, 2009).

The mammalian class C Vps protein Vps33a/b assembles into a core complex of class C Vps proteins including Vps11, Vps16, and Vps18. This core associates with Vps39 and Vps41 to form the HOmotypic fusion and Protein Sorting (HOPS) complex (Kim *et al.*, 2001; Nickerson *et al.*, 2009; Zhu *et al.*, 2009). The class C Vps core complex could also associate with Vps8/KIAA0804 and Vps3/TGFBRAP1 to constitute a hypothetical mammalian CORVET complex, a molecular species so far only documented in yeast (Peplowska *et al.*, 2007; Markgraf *et al.*, 2009). Class C core subunits and accessory HOPS subunits are critical for fusion events at the vacuole, a lysosome equivalent in the yeast *S. cerevisiae*. In this organism, HOPS orchestrates interactions with the GTPase ypt7, a rab7 ortholog, SNARES, and, recently, AP-3 to achieve selective membrane fusion (Ostrowicz *et al.*, 2008; Angers and Merz, 2009; Nickerson *et al.*, 2009; Wickner, 2010). Association of AP-3 and HOPS occurs at the vesicle fusion step with the vacuole when incoming Golgi-derived AP-3–coated vesicles reach the vacuole, the compartment where HOPS complexes reside in yeast (Angers and Merz, 2009).

Here we show that mammalian Vps class C/HOPS subunits coimmunoprecipitated and/or colocalized with the endosomal coats clathrin, AP-3, and Hrs. Isolated clathrin-coated vesicles had Vps class C/HOPS subunits on them, yet they were depleted of Hrs. We also found that acute perturbation of clathrin dynamics on and off membranes using FKBP–clathrin light chain (CLC) chimeras (Moskowitz *et al.*, 2003; Deborde *et al.*, 2008) altered the distribution of class C Vps/HOPS proteins in two different types of mammalian cells. HEK293T cells with reduced clathrin function had elevated levels of Vps class C proteins in rab5-positive endosomes, suggesting that clathrin dynamics at vesicular AP-3– or nonvesicular Hrs-positive endosomal domains regulate Vps class C protein content on early endosomes. We hypothesized that coats in endosomal tether-coat complexes could contribute to polarized distribution of tethers, such as the HOPS complex. In support of this idea, differentiated neuroendocrine cells accumulated Vps class C/HOPS subunits at the growing tip of processes, where they were concentrated with clathrin. Targeting of Vps class C/HOPS subunits from cell bodies to neurites was sensitive to clathrin function perturbation. Our data suggest that vertebrate cells differ from yeast in that the vertebrates engage in novel interactions between class C Vps–containing tethers and coats, perhaps for specialized demands such as polarized targeting in neuroendocrine and epithelial cells.

RESULTS

Subunits of the Vps class C/HOPS tethering complexes associate with clathrin–AP-3 adaptor subunits

We initially explored molecular interactions between tethering complexes and coats taking advantage of protein complexes affected in HPS. Mouse mutations on genes encoding the class C-Vps protein Vps33a or AP-3 subunits trigger a phenotype that recapitulates HPS (Suzuki *et al.*, 2003; Li *et al.*, 2004), suggesting that AP-3 and complexes containing Vps33a act on a common pathway. Consistent with this interpretation, subunits of the tethering HOPS complex interact with AP-3 in both *S. cerevisiae* (Angers and Merz, 2009) and mammalian cells (Salazar *et al.*, 2005, 2009). Despite this similarity, in mammalian cells, but not yeast, AP-3 shows interactions with clathrin (Seeger and Payne, 1992; Dell'Angelica *et al.*, 1998; Anand *et al.*, 2009). This observation suggests that Vps class C/HOPS tethers interact with coats differently in vertebrates as compared with yeast.

We tested whether all four class C Vps proteins, class C Vps33a-b isoforms, and the two HOPS-specific subunits associated with AP-3 and clathrin complexes isolated from HEK293T cells. As described in *Materials and Methods*, we used in vivo cross-linking with dithiobissuccinimidyl propionate (DSP) coupled to immunoaffinity chromatography with monoclonal antibodies (mAbs) against the AP-3 δ subunit or clathrin chains. DSP treatment decreases immunoreactivity of AP-3 δ subunit detected with a mAb against δ adaptin (see *Materials and Methods*). Vps class C and HOPS subunits present in AP-3 or clathrin immune complexes were detected with antibodies either against endogenously expressed Vps33b or tags engineered in recombinantly expressed subunits (Vps11, Vps16, Vps18, Vps33a, Vps33b, Vps39, and Vps41). We expressed tagged recombinant proteins because available class C Vps or HOPS subunit antibodies failed to detect endogenous proteins in multiple cell types, including HEK293T cells (our unpublished data).

We first determined whether phenotypic similarities between mice carrying mutations in either the class C Vps protein Vps33a or AP-3 subunits were predictors of a biochemical interaction between Vps33a and AP-3. Recombinantly expressed Vps33a selectively coprecipitated with AP-3 immunocomplexes (Figure 1A, compare lanes 3 and 5). This association was not restricted to Vps33a; similar results were obtained with tagged Vps33b (Figure 1A, compare lanes 4 and 6). The association of Vps33 isoforms with AP-3 could be due either to isolated Vps33 polypeptides interacting with AP-3 or Vps33 assembled into a Vps class C protein complex, such as HOPS. To discern between these hypotheses, we explored whether protein constituents of the HOPS complex were coisolated with AP-3 complexes together with endogenous Vps33b. Recombinantly expressed class C Vps proteins (Vps11, Vps16, and Vps18) or HOPS-specific subunits (Vps41 and Vps39) copurified with AP-3 and the endogenously expressed class C Vps protein, Vps33b. These associations were preferentially detected in the presence of DSP (Figure 1A, lanes 5 and 6; Figure 1B, lanes 8 and 10; Figure 1C, lane

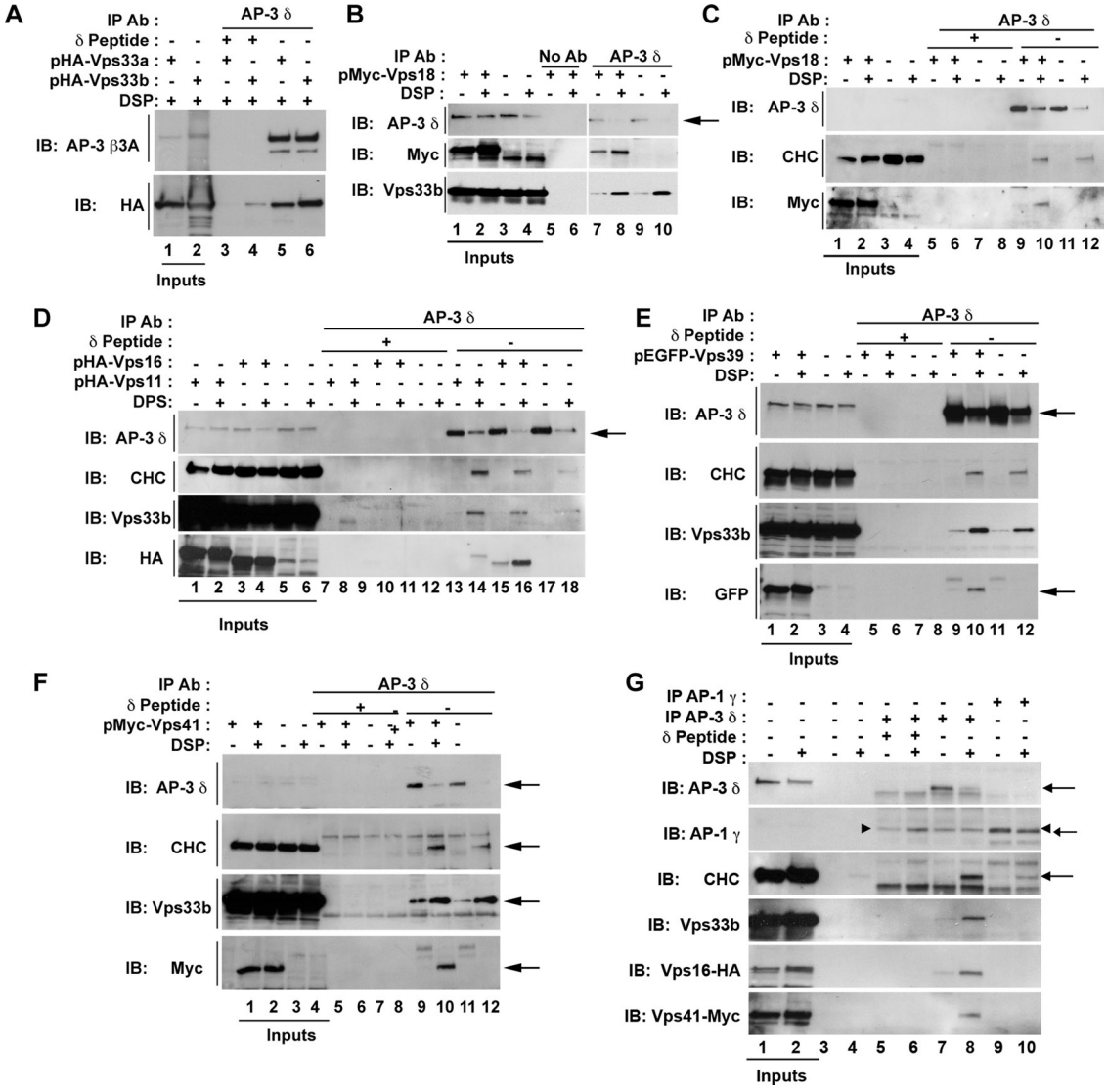

FIGURE 1: Association of class C Vps/HOPS subunits with the adaptor complex AP-3. HEK293T cells or cell lines expressing recombinant class C Vps/HOPS subunits (A–G) were left untreated (B–G, odd lanes) or treated (B–G, even lanes) with DSP at 4°C. Detergent-soluble cell extracts were incubated with sheep anti–mouse IgG-coated magnetic beads as follows: (A) Extracts of DSP-treated HEK293T cells transfected with Vps33A (odd lanes) or Vps33b (even lanes) incubated with magnetic beads decorated with antibody directed against AP-3 δ (lanes 3–6). The peptide used to raise the AP-3 δ mAb was added in excess during the immunoprecipitation to determine the specificity of signals detected by immunoblot (lanes 3 and 4). (B) Extracts of HEK293T cells (lanes 3, 4, 9, and 10) and cells expressing Vps18–Myc (lanes 1, 2, and 5–8) were incubated with anti–mouse IgG magnetic beads either lacking mouse antibody (lanes 5 and 6, No antibody) or linked to mouse mAb directed against AP-3 δ (lanes 7–10). (C) Extracts of HEK293T cells (lanes 3, 4, 7, 8, 11, and 12) and cells expressing Vps18–Myc (lanes 1, 2, 5, 6, 9, and 10) were incubated with anti–mouse IgG magnetic beads decorated with antibody directed against AP-3 δ (lanes 5–12). The peptide used to raise the AP-3 δ mAb was used as in A (lanes 5–8). (D) Extracts of HEK293T cells (lanes 5, 6, 11, 12, 17, and 18), cells expressing Vps16–HA (lanes 3, 4, 9, 10, 15, and 16), or cells expressing Vps11–HA (lanes 1, 2, 7, 8, 13, and 14) were incubated with anti–mouse IgG magnetic beads decorated with antibody directed against AP-3 δ (lanes 7–18). Peptide competition was performed as in A (lanes 7–12). (E and F) Extracts of HEK293T cells (E and F lanes 3, 4, 7, 8, 11, and 12) and cells expressing Vps39–GFP (E lanes 1, 2, 5, 6, 9, and 10) or cells expressing Vps41–Myc (F lanes 1, 2, 5, 6, 9, and 10) were incubated with anti–mouse IgG magnetic beads bound to AP-3 δ antibodies (E and F lanes 5–12). AP-3 δ peptide competition was performed as in A (E and F lanes 5–8). (G) Cells expressing both Vps16–HA and Vps41–Myc were incubated with anti–mouse IgG magnetic beads only (lanes 3 and 4) or beads decorated with mAbs directed against: AP-3 δ subunit (lanes 5–8, AP-3 δ) or AP-1 γ subunit (lanes 9 and 10, AP-1 γ). Specificity of association with AP-3 complexes was determined by peptide competition as in A (lanes 5 and 6). Immune complexes were resolved by SDS–PAGE, and their composition was assessed by immunoblot with antibodies against AP-3 δ, AP-3 β3A, AP-1 γ, CHC, endogenous Vps33b, Myc, GFP, or HA tags. Arrows in B, D, E, and F depict specific bands, and other bands correspond to background sheep or mouse IgG from beads or residual signal from previous immunoblot probings. Arrowhead in AP-1 γ blot strip depicts sheep or mouse IgG from beads or residual signal from previous immunoblot probing. All experiments were performed at least twice in stably or transiently expressing cells. For A–G, inputs represent 5%.

10; Figure 1D, lanes 14, 16, and 18; Figure 1, E and F, lanes 10 and 12). The association specificity of AP-3 and these Vps subunits was probed using magnetic beads conjugated with anti–mouse immunoglobulin (Ig)G (beads alone, Figure 1B). Vps18-Myc and Vps33b coisolated with AP-3 when these beads contained mouse AP-3 δ antibodies, yet none of these proteins were detected with beads alone (Figure 1B, compare lanes 5 and 6 with 7–10). Second, we out-competed AP-3 δ binding to magnetic beads linked to mouse δ-antibodies with the δ peptide antigen (Salazar *et al.*, 2009). We monitored peptide competition by assessing the presence of AP-3 subunits (β3A or δ) and clathrin heavy chain (CHC; an AP-3 binding partner) in immunoisolated cross-linked AP-3 complexes (Dell'Angelica *et al.*, 1998; Salazar *et al.*, 2009). Pretreating beads displaying δ-antibodies with the δ-peptide abolished binding of AP-3 subunits, clathrin, and all Vps subunits to these beads (Figure 1A, compare lanes 3 and 4 with lanes 5 and 6; Figure 1, C, E, and F, compare lanes 6 and 8 with 10 and 12; Figure 1D, compare lanes 8, 10, and 12 with lanes 14, 16, and 18). Abolished binding indicates that class C Vps and HOPS subunits interact with the beads by binding to intact AP-3 and not via some nonspecific mechanism. As a control, we showed that AP-1 complexes were not cross-linked to Vps33b, Vps16-HA (hemagglutinin), or Vps41-Myc, showing that the association of class C Vps and HOPS subunits with AP-3 was selective (Figure 1G). AP-3-Vps subunit associations could result simply from abundantly expressed tagged proteins in endosomal compartments. To test this hypothesis, we asked whether the Vps33b-interacting protein Spe39 coisolates with AP-3 and clathrin complexes. We selected Spe39 because we previously demonstrated that Spe39 defines a subclass of Vps class C/HOPS complexes (Zhu *et al.*, 2009). In fact, Spe39 is present in a discrete pool of the total Vps33b and other class C protein as determined by quantitative immunomicroscopy (Zhu *et al.*, 2009). Importantly, endogenous Spe39 does not colocalize with AP-3 or CLCs (Supplemental Figure 1, A and B). Consistent with our immunomicroscopy, neither endogenous nor recombinant green fluorescent protein (GFP)-tagged Spe39 coprecipitated with AP-3 immunocomplexes (Supplemental Figure 1, C and D). These results argue against nonselective DSP cross-linking of recombinantly expressed proteins to AP-3.

Others have proposed that the HOPS subunit Vps41 can associate with AP-3 as a clathrin-like coat (Rehling *et al.*, 1999; Darsow *et al.*, 2001). Consequently, we next looked for association of clathrin with Vps class C/HOPS in AP-3 cross-linked complexes. Cross-linked samples were treated with antibodies against CLC. Both Vps33 isoforms selectively coisolated with clathrin complexes isolated with CLC antibodies (Figure 2A, lane 3). We found that CLC consistently coimmunoprecipitated with CHC, the AP-3 δ subunit, endogenous Vps33b, and Vps41-Myc (Figure 2B, lane 7). Neither coats nor Vps proteins were detected with beads alone or beads coated with nonimmune IgG (Figure 2A, compare lanes 3 and 5 with lane 7). Immunoprecipitation of CLC after siRNA-mediated down-regulation of CHC not only showed lowered CHC levels, but also greatly diminished the abundance of the AP-3, Vps33b, and Vps41-Myc proteins (Figure 2B, compare lanes 7 and 8). We further assessed whether clathrin, AP-3, and Vps41-Myc form a complex together by performing sequential immunopurification of clathrin-containing AP-3 complexes from HEK293T cells stably expressing Vps41-Myc (Figure 2C). First, cross-linked AP-3 complexes were immunoaffinity purified with AP-3 δ antibodies in either the absence or presence of δ antigenic peptide as a control of binding selectivity to beads (Figure 2C, compare lanes 3 and 4 with lanes 5 and 6). Cross-linked AP-3 complexes bound to beads (Figure 2C, lane 6) were then eluted in native conditions from magnetic beads using the δ antigenic peptide. These eluted AP-3-cross-linked complexes were subjected to a second round of immunomagnetic isolation with either nonimmune mouse IgG (control) or a monoclonal anti-CLC. The composition of complexes bound to CLC antibody-coated beads was assessed by immunoblot. CLC antibodies allowed coimmunoprecipitation of the AP-3 δ subunit and Vps41-Myc (Figure 2C, compare lanes 7 and 8), indicating that at least a subset of AP-3, clathrin, and the HOPS subunit Vps41 exist in a multiprotein complex.

The HOPS subunit Vps41 is known to directly interact with AP-3 through its δ subunit in yeast, whereas mammalian CHC interacts with AP-3 through its β3 subunit (Dell'Angelica *et al.*, 1998; Rehling *et al.*, 1999; Angers and Merz, 2009). These interactions suggest that AP-3 could bridge between the HOPS complex and clathrin in mammalian cells. We examined this possibility by performing shRNA down-regulation of either AP-3 δ or CHC, cross-linking in vivo with DSP, and immunoprecipitating cell extracts with CLC or AP-3 δ antibodies (Figure 2, D and E). As compared with control cells, AP-3 δ subunit shRNA treatment caused a ~50% drop in the level of AP-3 δ polypeptide (49 ± 4.6%), whereas CHC shRNA eliminated nearly all CHC (95.5 ± 0.9% reduction, n = 4, Figure 2, D and E, compare lanes 1 and 2). Immunoaffinity purification with CLC antibodies from mock shRNA treated control cells recovered clathrin complexes that were cross-linked to AP-3 subunits, Vps33b, and Vps41-Myc (and Vps39; unpublished data) (Figure 2D, lane 5). Although CLC antibodies failed to isolate AP-3 subunits from AP-3 δ shRNA-treated cells, there were no discernible effects on the levels of Vps33b or Vps41-Myc present in CLC-isolated cross-linked complexes (Figure 2D, compare lanes 5 and 6). These results suggest that other tetrameric adaptors, such as AP-1, could mediate the association between Vps class C and HOPS subunits with clathrin. We did not detect, however, an association of Vps class C or HOPS subunits to cross-linked AP-1 complexes isolated from HEK293T cells (Figure 1G). Furthermore, cross-linked AP-3 complexes isolated from CHC-depleted cells, although devoid of clathrin, contained both endogenous Vps33b and recombinantly expressed Vps41-Myc (Figure 2E, compare lanes 8 and 10) or Vps39-GFP (unpublished data). In fact, cross-linked AP-3 complexes isolated from CHC shRNA–treated cells copurified with increased levels of Vps41-Myc and Vps33b. This effect may be attributable to an increased expression of Vps41-myc but not Vps33b in CHC-shRNA–treated cells (Figure 2E, compare lanes 1 and 2; Vps41-Myc 255 ± 18.5% of control shRNA, n = 2; Vps33b 138.5 ± 42%, n = 4). These data indicate that, despite the fact that clathrin–AP-3–HOPS subunits form a complex, clathrin is not required for the binding of Vps class C and HOPS subunits to AP-3 complexes, nor is AP-3 necessary for their binding to clathrin complexes. In addition to AP-3, other clathrin-interacting molecules present in endosomes may interact with Vps class C/HOPS subunits. One such mechanism is the Hrs-clathrin flat coat present in endosomes (Raiborg *et al.*, 2002, 2006). Endogenous Hrs or recombinantly expressed Hrs-Myc coprecipitated endogenous CHC and Vps33b (Figure 2F, lanes 5–6 and 5′-6′). These interactions were selective as judged by the absence of Vps33b and CHC in GFP control immunoprecipitations as well as by the absence of transferrin receptor in all immunocomplexes (Figure 2F, lanes 3–4 and 3′-4′). Collectively, our results indicate that Vps class C/HOPS subunits copurify with at least two pools of clathrin present in early endosomes: clathrin–AP-3 and clathrin–Hrs complexes.

Vps class C and HOPS subunits are present in clathrin-coated organelles

Vps class C and HOPS subunits association with clathrin–AP-3 and clathrin–Hrs predicts that these Vps proteins should be present in

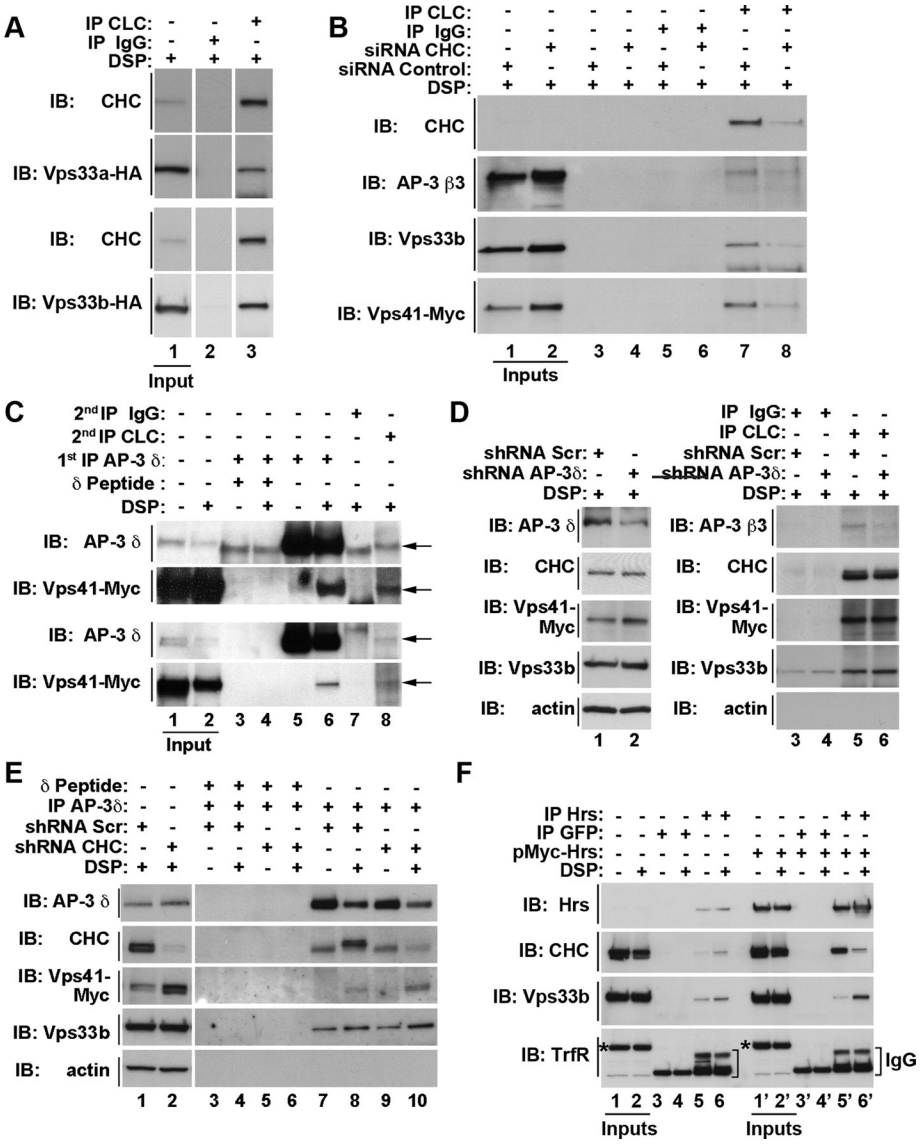

FIGURE 2: CHC and CLC associate with class C Vps/HOPS subunits. (A) Extracts of DSP-treated HEK293T cells transfected with Vps33A or Vps33b were incubated with magnetic beads decorated with antibody directed against control IgG (lane 2) or CLC (lane 3). Immunocomplexes were resolved by SDS–PAGE, and contents were analyzed by immunoblot with antibodies against the HA tag and CHC. Input represents 5%. (B) HEK293 cells stably expressing Vps41–Myc were treated with scramble (Control, odd lanes) and CHC siRNA (CHC, even lanes) for 5 d. siRNA-treated cells were incubated in the presence of DSP (all lanes) at 4°C. Detergent-soluble cell extracts were immunoprecipitated with magnetic beads lacking mouse IgG (lanes 3 and 4), control mouse IgG (monoclonal SV2 lanes 5 and 6), or antibodies against CLCs (lanes 7 and 8). Immunocomplexes were resolved by SDS–PAGE, and contents were analyzed by immunoblot with antibodies against CHC, AP-3 β3A, Vps33b, and Myc. Depletion of CHC prevents the precipitation of Vps33b and Vps41-Myc with CLC. Input represents 5%. (C) Vps41–Myc is in a complex with AP-3 and clathrin complexes. HEK293T cells stably expressing Vps41–Myc were treated in the absence (lanes 1, 3, and 5) or presence of DSP (lanes 2, 4, and 6–8). Clarified cell extracts were first immunoprecipitated with magnetic beads decorated with AP-3 δ antibodies (lanes 3–6) either in the absence (lanes 5 and 6) or presence of excess δ antigenic peptide as a control (lanes 3 and 4). Cross-linked AP-3 complexes bound to beads in lane 6 were eluted under native conditions using δ antigenic peptide. These eluted cross-linked AP-3 complexes were subjected to a second round of immunoprecipitations with control mouse IgG (mAb SV2 [top two panels] and SY38 [bottom two panels], lane 7) or CLC antibodies (lane 8). SV2 and SY38 antibodies recognize neuronal antigens absent in HEK293T cells. Immunocomplexes were resolved by SDS–PAGE, and contents were analyzed by immunoblot with antibodies against AP-3 δ and Myc epitope. Arrows mark specific bands for AP-3 δ and Vps41–Myc. Note the different background bands obtained with the two different negative control antibodies during the second round of immunoprecipitation. Input represents 5%. (D) Interaction of Vps class C/HOPS subunits with clathrin is not affected by down-regulation of AP-3. HEK293T cells stably expressing Vps41–Myc were infected with lentiviruses encoding nontargeting shRNA (Scr, lanes 1, 3, and 5) or shRNA targeting AP-3 δ (lanes 2, 4, and 6). After 6 d, cells were incubated in the presence of DSP (lanes 1–6) and homogenized. Detergent cell extracts were immunoprecipitated with magnetic beads decorated with control mouse IgG (monoclonal SY38, lanes 3 and 4), or antibodies against CLCs (lanes 5 and 6). Immunocomplexes were resolved by SDS–PAGE, and contents were analyzed by immunoblot with antibodies against AP-3 β3A, AP3 δ, CHC, Myc epitope, Vps33b, and β actin. Lanes 1 and 2 correspond to homogenates run on different gels to assess efficiency of down-regulation. (E) Vps class C/HOPS subunits interaction with AP-3 is not affected by down-regulation of CHC. HEK293T cells stably expressing Vps41–Myc were infected with lentiviruses encoding nontargeting shRNA (Scr, lanes 1, 3, 4, 7, and 8) or shRNA targeting CHC (lanes 2, 5, 6, 9, and 10). After 6 d, cells were incubated in the absence (lanes 3, 5, 7, and 9) or presence of DSP (lane 1 and even lanes). Cell extracts were immunoprecipitated with magnetic beads decorated with AP-3 δ antibodies (lanes 3–10) either in the absence (lanes 7–10) or presence of an excess of δ antigenic peptide as a control (lanes 3–6). Immunocomplexes were resolved by SDS–PAGE, and contents were analyzed by immunoblot with antibodies against AP-3 δ, CHC, Myc epitope, Vps33b, and β actin. Lanes 1 and 2 correspond to homogenates run on different gels to assess efficiency of down-regulation. (F) Vps33b associates with clathrin–Hrs coats. HEK293T cells (lanes 1–6) or transiently transfected with Hrs–Myc (lanes 1′–6′) were treated in the absence (odd lanes) or presence of DSP (even lanes). Detergent-soluble cell extracts were immunoprecipitated with magnetic beads decorated with GFP antibodies as controls (all lanes 3 and 4) or Hrs antibodies (all lanes 5 and 6). Immunocomplexes were resolved in SDS–PAGE, and their composition was analyzed by immunoblot with antibodies against Hrs, CHC, Vps33b, and transferrin receptor (TrfR) as control. Asterisks denote TrfR band, and brackets denote IgGs. Inputs correspond to 5%.

domains of early endosomes as well as clathrin-coated vesicle carriers. The presence of Vps class C and HOPS subunits in early endosomes and clathrin-coated carriers would be consistent with the observation that AP-3, AP-3–clathrin budding profiles, clathrin–Hrs flat coats, Vps class C, and HOPS subunits are found in early endosomal compartments (Raiborg *et al.*, 2002, 2006;

Peden *et al.*, 2004; Richardson *et al.*, 2004; Theos *et al.*, 2005). We determined the subcellular distribution of Vps class C and HOPS subunits by immunofluorescence using quantitative Delta deconvolution microscopy. We used antibodies against coats (clathrin, AP-1 γ, and AP-3 δ) and either the early endosome marker, rab5, or the late endosomal markers rab7, rab7b, and LAMP-1. Our rationale for including the late endosomal marker rab7b is that its depletion selectively increases the protein levels of AP-3 (Progida *et al.*, 2010). We focused on endogenously expressed Vps33b and used Vps16-HA to further validate Vps33b results. In addition, we analyzed the subcellular localization of the HOPS subunits Vps39–GFP and Vps41–Myc in clathrin-positive compartments and endosomes. Endogenous Vps33b partially overlapped with puncta positive for AP-3 (Figure 3, B and C) and/or clathrin (Figure 3, E and F). Although partial, of these two coats, fluorescent signal overlap was more pronounced between Vps33b and clathrin than Vps33b with AP-3. One third of all Vps33b-positive pixels were positive for CHC (Figure 3, E, F, and J). Similar to Vps33b, Vps16-HA was preferentially found in puncta positive for CHC (Figure 3, G and J) or AP-3 δ (Figure 3H), where coats signals partially overlapped with class C Vps subunits. In contrast to CHC localization, Vps33b and Vps16-HA signals minimally overlapped with AP-1 γ (Figure 3, I and J).

Vps33b was found in rab5 endosomes, in which we observed a partial overlap of fluorescent signals (Figure 3, A and J). In contrast, Vps33b was undetectable in late endosomes defined by rab7 and LAMP-1 staining (Figure 3J). Vps33b overlapped with rab7b (Figure 3, D and J), however, at levels similar to those of AP-3 (Figure 3J). Rab7b organelles were also positive for clathrin and the late endosomal SNARE vesicle-associated membrane protein 7 (VAMP7; Figure 3J). Another class C Vps protein, Vps16–HA, showed a similar pattern of endosomal localization compared with Vps33b (Figure 3J). Analysis of the distribution of the HOPS subunits Vps41–Myc and Vps39–GFP revealed that the signal overlap with coats and endosomal markers was far less pronounced as compared with the class C Vps proteins Vps33b/Vps16–HA. Nonetheless, the two HOPS-specific Vps subunits, Vps41–Myc and Vps39–GFP, were localized to rab5- and CHC-positive compartments (Figure 3J).

The partial overlap between coats, Vps class C, and HOPS proteins suggests that domains of endosomes, rather than the whole organelle, contain these factors. We tested this hypothesis by enlarging rab5 compartments expressing the GTPase-deficient rab5Q79L. This tool has been successfully used to enlarge endosomes facilitating the identification of domains in the limiting membrane of endosomes by high-resolution optical microcopy (Raiborg *et al.*, 2002, 2006; Craige *et al.*, 2008). We determined the distribution of coats, HOPS subunits, and class C Vps proteins by deconvolution immunofluorescence microscopy and volume rendering of digitally reconstructed enlarged endosomes (Figure 4 and Supplemental Movies 1 and 2). Single optical sections revealed that endogenous Vps33b, Vps16–HA, and Vps41–Myc were present in the limiting membrane of enlarged rab5 endosomes in discrete domains often partially overlapping with either CHC- or AP-3 δ–decorated patches (Figure 4). Fifty and thirty-five percent of all Vps33b domains present on the limiting membrane of rab5Q79L-enlarged endosomes were positive for CHC and AP-3 δ subunit, respectively (52.4 ± 25.7, n = 68; 34.2 ± 24.3, n = 103). Digital volume rendering of rab5Q79L-enlarged endosomes confirmed that the HOPS subunit Vps41–Myc was present in discrete domains that partially overlapped either with CHC (Supplemental Movie 1) or AP-3 δ (Supplemental Movie 2) at the limiting membrane of enlarged endosomes.

We isolated clathrin-coated vesicles from HEK293T cells or HEK293T cells stably expressing either Vps41–Myc or Vps16–HA and asked whether class C Vps/HOPS proteins were present in these organelles (Figure 5 and Supplemental Figure 2). Clathrin-coated vesicle isolation was monitored by the enrichment of CHC detected by Coomassie Blue dye (Figure 5A) or by immunoblot with antibodies CHC, AP-1 γ, AP-2 α, and AP-3 β3 subunits in clathrin-coated vesicle fractions (Figure 5B and Supplemental Figure 2, compare lanes 1 and 6). Clathrin-coated vesicles contained class C Vps proteins Vps33b and Vps16–HA and the HOPS subunit Vps41–Myc (Figure 5B and Supplemental Figure 2, compare lanes 1 and 6). Of these Vps proteins, Vps41–Myc and Vps16–HA were clearly enriched in clathrin-coated vesicle fractions. We isolated clathrin-coated vesicles from control or CHC RNAi–treated cells to define whether Vps class C and HOPS subunits cosedimenting with clathrin-coated vesicles correspond to true components of these carriers or just contaminants present on these membranes (Borner *et al.*, 2006). Coomassie Blue staining revealed that clathrin-coated vesicle fractions isolated from CHC down-regulated cells decreased the content of several polypeptides, including CHC (Figure 5A, asterisks). Down-regulation of CHC precluded formation of clathrin-coated vesicles as determined by the absence or decreased levels of adaptor subunits from clathrin-coated vesicles (Figure 5B; Supplemental Figure 2, compare lanes 6 and 6′; Figure 5C). Importantly, the levels of Vps33b, Vps16–HA, or Vps41–Myc were significantly reduced from clathrin-coated vesicles isolated from CHC RNAi–treated cells indicating that Vps33b, Vps16–HA, and Vps41–Myc specifically reside in clathrin-coated vesicles (Figure 5B; Supplemental Figure 2, compare lanes 6 and 6′; Figure 5C). Contamination of clathrin-coated vesicle fractions with early endosomes markers such as EEA1, rabaptin5, and Hrs was negligible (Figure 5B). Therefore these results indicate that clathrin, Vps class C, and HOPS subunits coreside both in coated domains of early endosomes as well as clathrin-coated vesicle carriers.

Acute perturbation of clathrin alters Vps class C/HOPS subunit subcellular distribution

We evaluated the effect of CHC shRNA on the distribution of Vps class C/HOPS subunits in rab5- and rab7b-positive endosomes. CHC down-regulation, which is achieved within several days of shRNA treatment, did not alter the distribution of Vps class C/HOPS subunits in rab5 or rab7b compartments, suggesting compensatory mechanisms controlling Vps class C/HOPS subunit subcellular distribution (unpublished data). To overcome possible compensatory mechanisms, we acutely perturbed clathrin function by using a chemical/genetic approach that uses chimeric CLCs carrying an oligomerization module, a modified FKBP 12 domain (Moskowitz *et al.*, 2003; Deborde *et al.*, 2008). FKBP domains selectively oligomerize upon addition of the cell-permeant bivalent chemical AP20187. CLC oligomerization that follows incubation with AP20187 halts vesicle formation from donor organelles, such as plasma membrane or *trans*-Golgi network by "freezing" clathrin onto membranes and aborted budding profiles (Moskowitz *et al.*, 2003; Deborde *et al.*, 2008). Thus we used FKBP–CLC chimeras to trap clathrin at membranes. Tagged FKBP–CLC chimeras incorporated into 60.7 ± 18.5% (n = 30) of all CHC-positive organelles in HEK293T cells as determined by deconvolution microscopy (Supplemental Figure 3A). Like endogenous CLC (Figure 2), chimeric mCherry-FKBP–CLC specifically coprecipitated class C Vps/HOPS subunits (Supplemental Figure 3D). Cell treatment with AP20187 for 2 h induced enlargement of CHC/tagged-FKBP–CLC dual-labeled organelles and the accumulation of endogenous and recombinant clathrin chains at the perinuclear region (Supplemental Figure 3, B and C). The perinuclear accumulation of CHC in

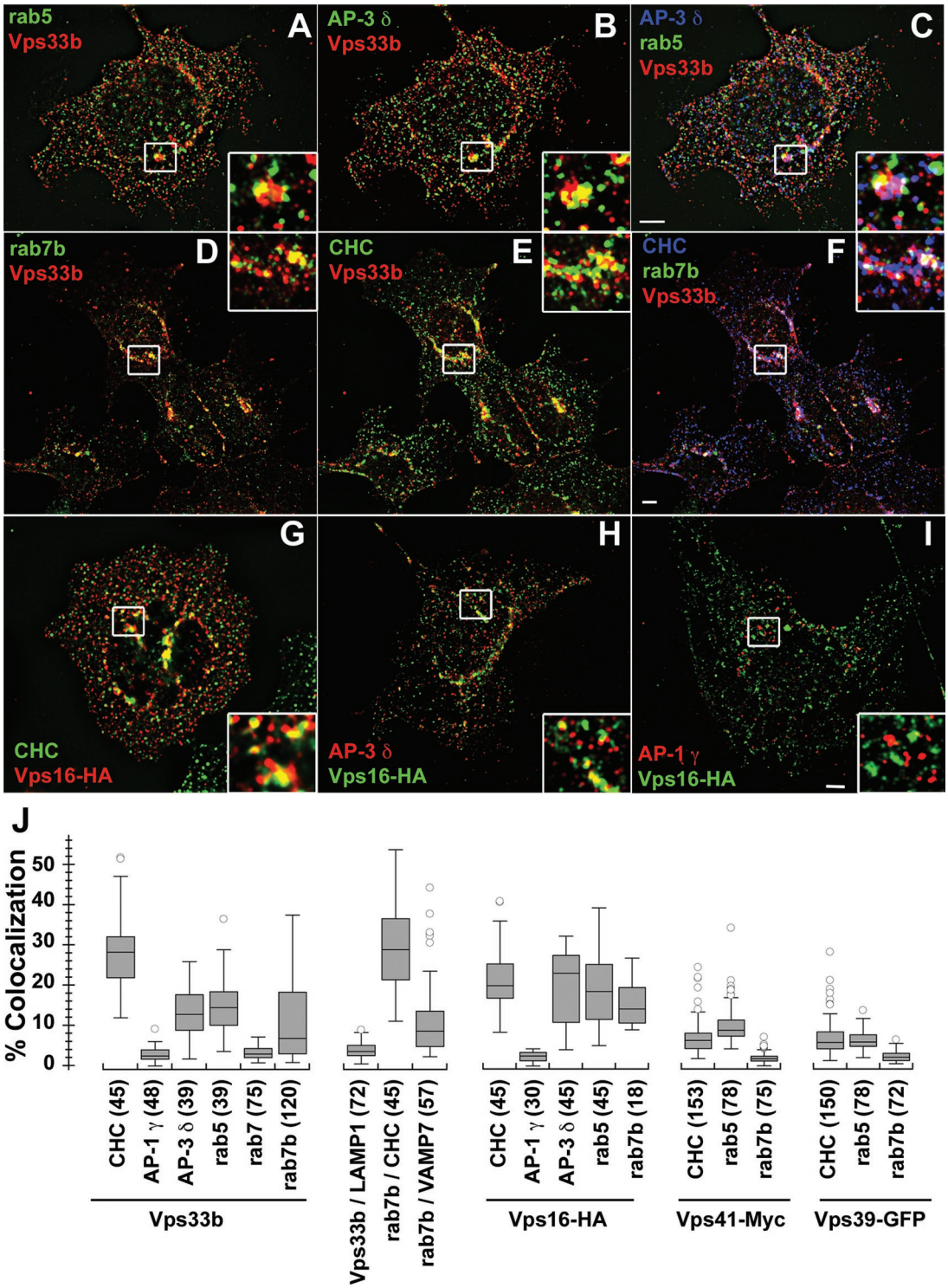

FIGURE 3: Vps class C/HOPS are present in AP-3, clathrin, Rab5, and Rab7b-compartments. HEK293T cells were fixed, and either triple (A–F) or double (G–I) labeled for indirect immunofluorescence with antibodies against the following antigens: Vps33b, rab5, and AP-3 δ (A–C); Vps33b, rab7b, and CHC (D–F); HA epitopes to detect recombinantly expressed Vps16-HA (G–I), and either CHC (G), AP-3 δ (H), or AP-1 γ (I). Cells were imaged by Delta deconvolution fluorescence microscopy. Bar depicts 5 μm; images to the right are 300% magnifications of white-boxed inserts. (J) Quantitative analysis of Vps class C/HOPS subcellular distribution. HEK293T cells or those expressing recombinant Vps16–HA, Vps39–GFP, or Vps41–Myc were labeled with combinations of antibodies against endogenous Vps33b or tags engineered in the Vps class C/HOPS subunits Vps16, Vps39, Vps41; the coats CHC, AP-1 γ, AP-3 δ; the early endosome marker rab5; the late endosome markers VAMP7, rab7, rab7b, and LAMP-1. Cells were imaged by Delta deconvolution fluorescence microscopy, and the percentage of overlapping pixels of different antigen combinations was determined using Metamorph. The number of images analyzed appears in parentheses, and quantifications were obtained in at least three independent experiments.

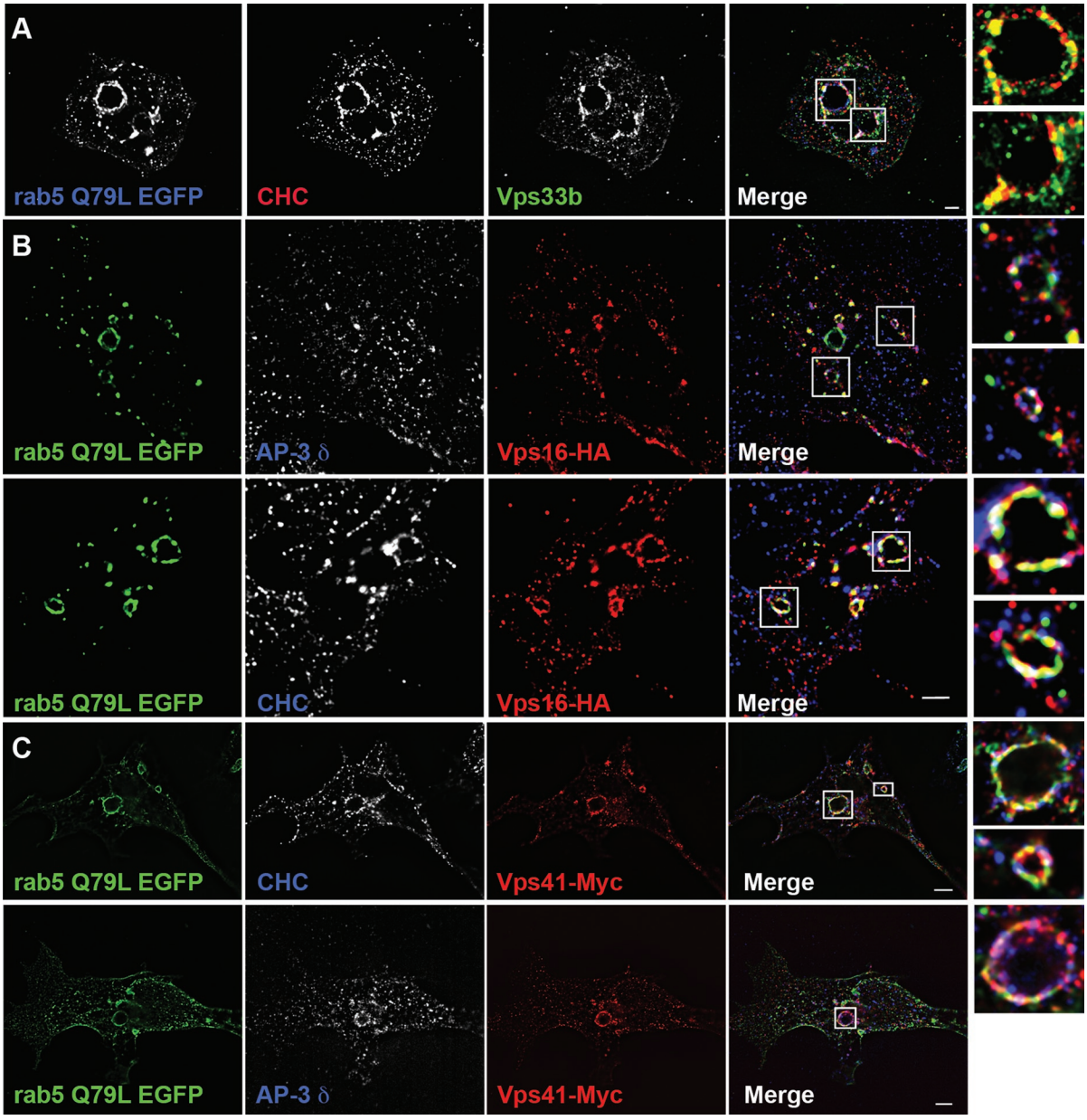

FIGURE 4: Vps class C/HOPS subunits localize to discrete domains of enlarged early endosomes. HEK293T cells transiently expressing recombinant rab5Q79L–GFP alone (A) or rab5Q79L–GFP plus either Vps16–HA (B) or Vps41–Myc (C) were fixed and triple labeled for indirect immunofluorescence with antibodies against GFP (A–C) plus: (A) antibodies against Vps33b and CHC, (B) antibodies against HA epitope plus either AP-3 δ or CHC, or (C) antibodies against Myc epitope plus either AP-3 δ or CHC. Cells were imaged by Delta deconvolution fluorescence microscopy. Bar depicts 5 μm; images to the right are 300% magnifications of insets. Supplementary Movies 1 and 2 depicts a tridimensional rendering of enlarged endosomes shown in panel C.

HEK293T cells indicates that clathrin-dependent processes are rapidly inhibited by FKBP–CLC chimeras (Moskowitz *et al.*, 2003; Deborde *et al.*, 2008).

We next determined the effect of chemically perturbing clathrin function in HEK293T- and NGF-differentiated PC12 cells on Vps class C/HOPS subunits (Figures 6–9 and Supplemental Movies 3–6). We determined the speed of the AP20187-induced Vps class C redistribution by in vivo, time-lapsed confocal microscopy. mCherry-FKBP-CLC– and Vps18-GFP–expressing cells were imaged 25 min before drug addition and for 2 h in the presence of AP20187. mCherry-FKBP–CLC oligomerization induced by AP20187 quickly caused an accumulation of recombinant clathrin and Vps18–GFP in the perinuclear region. Concomitantly, Vps18–GFP organelles distributed in the cell periphery grew in number and size (Figure 6C and Supplemental Movie 5 and 6). Vps18–GFP redistributed in <30 min after AP20187 addition and reached a plateau by 60 min. Addition of either AP20187 to cells expressing solely Vps18–GFP (Figure 6A and Supplemental Movie 3) or ethanol vehicle to mCherry-FKBP-CLC and Vps18-GFP doubly expressing cells (Figure 6B and Supplemental Movie 4) did not alter the subcellular distribution of either fluorescently tagged protein. These results demonstrate a swift rearrangement of class C Vps

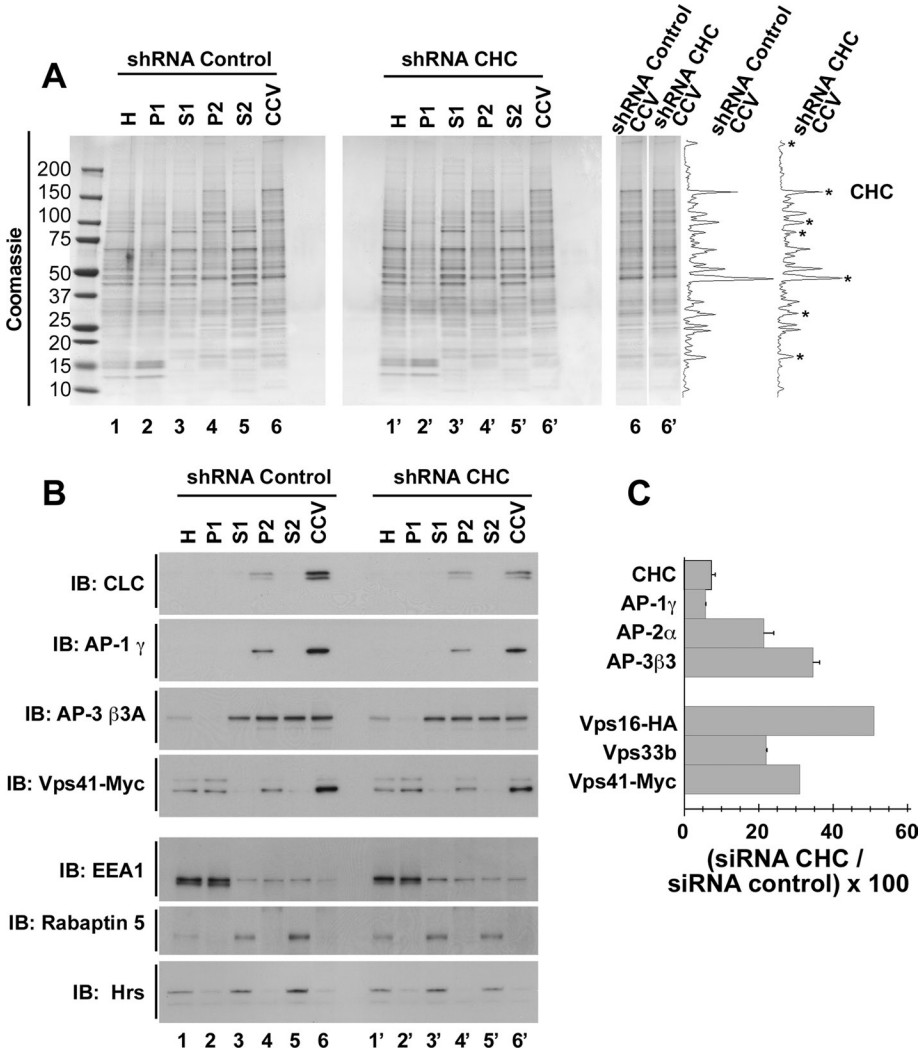

FIGURE 5: Vps class C/HOPS subunits cosediment with clathrin-coated vesicles. (A and B) HEK293T cells were infected with scramble (lanes 1–6) or CHC directed shRNA lentiviruses (CHC, lanes 1′–6′). Cells were homogenized, and clathrin-coated vesicle fractions were obtained (H, homogenate; P_n, pellets; S_n, supernatants; and CCV, clathrin-coated vesicle-enriched fraction). Fractions were Coomassie stained (A). Right panel in A depicts densitometry traces of lanes 6 and 6′ where protein bands decreased by CHC knock-down are marked by asterisks. (B) Shows the same fractions as in (A) blotted with antibodies against the coats AP-1 γ, AP-3 β3A, CLCs, and the HOPS subunit Vps41–Myc. Endosomal contamination was assessed by blotting with antibodies against EEA1, rabaptin 5, and Hrs. (C) Quantification of CCV fractions from immunoblot of the coat proteins AP-1 γ, AP-2 α, AP-3 β3A, AP-3 δ, CHC; and the Vps class C/HOPS subunits Vps16–HA, Vps33b, and Vps41–Myc. The content of these antigens was determined as a percentage between CHC and scrambled knockdowns. Data depict the quantification of three experiments.

proteins by acute chemical/genetic inhibition of clathrin-coated vesicle formation.

The effects of AP20187-induced perturbation of clathrin function were not just restricted to Vps18–GFP. Analysis of images from fixed specimens showed that drug addition caused redistribution of endogenous Vps33b, Vps18–GFP, or Vps41–Myc into larger puncta preferentially found at the perinuclear region as was seen with Vps18–GFP during live imaging (Figure 7). This change in Vps class C/HOPS subunits distribution occurred concomitantly with an increased colocalization of Vps class C/HOPS subunits with either CHC or mCherry-FKBP–CLC (Figure 7A). Importantly, AP20187 increased the colocalization of clathrin chains with AP-3 as well as rab5 and rab7b, suggesting that AP20187 similarly traps clathrin chains on both endosomes (Figure 7, B and C). These results are consistent with the presence of clathrin in AP-3–, rab5-, and rab7b-positive compartments, as was observed at steady state in HEK293T cells (Figure 3J).

Vps class C/HOPS subunit binding to both clathrin–AP-3 and clathrin–Hrs coats suggest that Vps class C/HOPS subunit accumulation should be preferentially observed in early endosomes as compared with other intracellular compartments, such as late endosomes or the *trans*-Golgi network. To test this hypothesis, we analyzed the affects of AP20187 on the colocalization of rab5, rab7b, and AP-1 with CHC and/or endogenous Vps33b in mCherry-FKBP-CLC–expressing cells using deconvolution microscopy. The amount of CHC-positive puncta that were also positive for Vps33b doubled from 12.3 ± 5.3% (n = 120) to 20.8 ± 11.9% after drug addition (n = 120, $p < 0.0001$, Wilcoxon–Mann–Whitney test; Figure 8). AP20187 increased the colocalization of Vps33b with rab5 from 10.2 ± 5% to 20 ± 9.6% (n = 60, $p < 0.0001$, Wilcoxon–Mann–Whitney test; Figure 8; Supplemental Figure 4, compare A and B). In contrast, colocalization between rab7b and Vps33b modestly decreased after 2 h of clathrin perturbation (Figure 8; Supplemental Figure 4, compare C and D). Vps33b colocalization with clathrin in rab5-positive endosomes was selective because overlap between Vps33b and AP-1 γ remained at background levels before or after AP20187 incubation (Supplemental Figure 5 and Figure 8). Although AP20187 induced clathrin recruitment to rab5- and rab7b-positive compartments to a similar extent (Figure 8), the preferential association of Vps33b- to rab5-positive organelles after drug-induced clathrin perturbation supports the hypothesis that clathrin coats selectively regulate the localization of class C Vps proteins to early endosomes.

Clathrin and Vps class C proteins are targeted to neuronal processes by clathrin-dependent mechanisms

We tested whether class C Vps proteins present in clathrin-coated organelles undergo directional delivery in polarized cells. To this end, we used human cortical neurons HCN-1A, a cell type that extends processes (Ronnett *et al.*, 1990), as well as NGF-differentiated PC12 cells. HCN-1A cells were double-labeled with antibodies against endogenous Vps33b and CHC, and cells were imaged by high-resolution Delta deconvolution microscopy (Figure 9A). Vps33b was concentrated at the tip of neuronal processes where it preferentially colocalized with clathrin. This polarized distribution of a class C Vps/HOPS subunit was also observed by in vivo imaging of NGF-differentiated PC12 cells expressing recombinant mCherry-FKBP–CLC with either Vps39–GFP (unpublished data) or Vps18–GFP (Figure 9B).

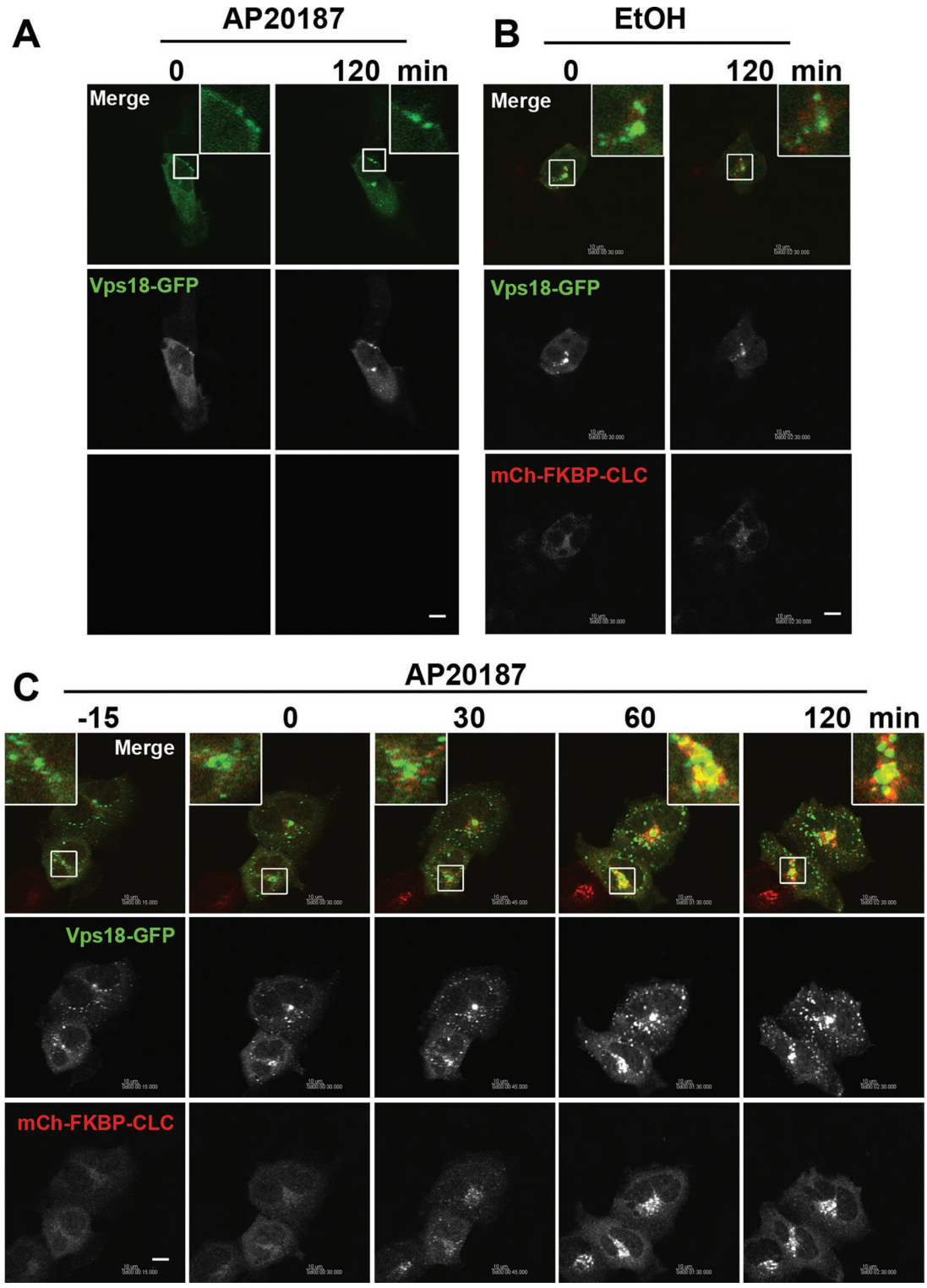

FIGURE 6: In vivo chemical/genetic disruption of clathrin chains rapidly redistributes Vps18. HEK293T cells transiently expressing Vps18–GFP (A) and an mCherry-tagged (mCh, B and C) chimeric CLC carrying a modified FKBP 12, as an oligomerization module, were imaged by time-lapse confocal microscopy in the presence of ethanol vehicle (B, EtOH, 0.05% vol/vol) or AP20187 (A and C, 50 nM). Cells were imaged for 25 min before vehicle or drug additions and continuously for 2 h after drug addition. AP20187 effects upon Vps18–GFP require expression of mCh-FKBP-CLC. AP20187 induces redistribution of Vps18–GFP in <30 min. See Supplemental Movies 3–6.

We predicted that if class C Vps proteins associate with clathrin-positive organelles generated at the cell body for subsequent delivery to neurites, then inhibition of clathrin-dependent mechanisms by AP20187 should lead to a progressive decrease of mCherry-FKBP–CLC and Vps18–GFP fluorescent signals in the proximal segment of neurites. NGF-differentiated PC12 cells expressing mCherry-FKBP–CLC and Vps18–GFP were treated with vehicle or with AP20187 and continuously imaged by confocal

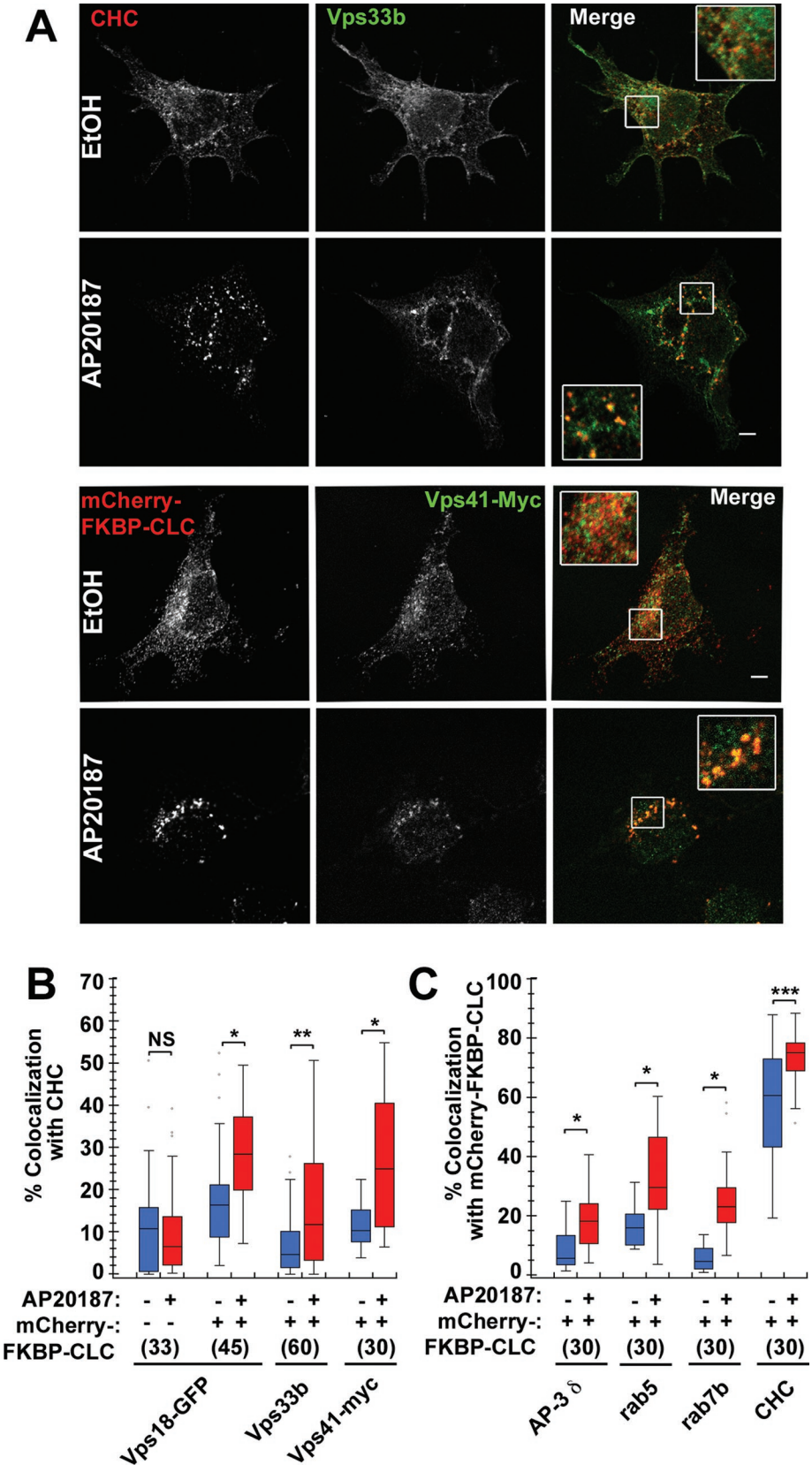

FIGURE 7: Chemical/genetic disruption of clathrin chains affects Vps class C/HOPS subunits and coat distribution. HEK293T cells transiently expressing mCherry-FKBP–CLC were treated in the presence of ethanol vehicle (EtOH, 0.05% vol/vol) or AP20187 (50 nM) for 2 h. Cells were fixed, processed for indirect immunofluorescence microscopy, and imaged by confocal microscopy. (A) Top two panels, cells expressing mCherry-FKBP–CLC were probed with antibodies against endogenous CHC and Vps33b. Bottom two panels, cells expressing mCherry-FKBP–CLC and Vps41–Myc were probed with antibodies against mCherry and Myc epitopes. Note the redistribution of clathrin chains and Vps class C/HOPS subunits. (B) HEK293T cells mock transfected (–) or expressing mCherry-FKBP–CLC (+) were treated in the presence of ethanol vehicle (–) or AP20187 (+) for 2 h. Cells were stained with antibodies against CHC and one of the following antigens: GFP, to detect exogenously expressed Vps18–GFP; Myc, to detect exogenously expressed Vps41–Myc; or Vps33b to detect the endogenous protein. (C) HEK293T cells expressing mCherry-FKBP–CLC (+) were treated in the presence of ethanol vehicle (–) or AP20187 (+) for 2 h. Cells were stained with antibodies against mCherry and one of the following: AP-3 δ, rab5, rab7b, or CHC. (B and C) Percentage of overlapping pixels between different antigen combinations was determined using Metamorph. Numbers depicted in parentheses denote numbers of analyzed images obtained from at least three independent experiments. NS, not significant; * $p < 0.0001$, ** $p < 0.003$, *** $p < 0.0004$, Wilcoxon–Mann–Whitney Rank Sum Test.

microscopy for 2 h. The integrated fluorescence intensity per volume unit was measured in the proximal third of the neurite (Figure 9B, arrows). Addition of AP20187 decreased CLC and Vps18 fluorescence in the proximal segment of neurites after 2 h (Figure 9B). Quantification of CLC and Vps18 fluorescence intensity revealed a progressive reduction per unit of proximal neurite volume after AP20187 incubation (Figure 9C, open circles). This decrease was not observed in vehicle-treated cells (Figure 9C, closed circles). Changes in fluorescence intensity per voxel induced by drug incubation are due to neither changes in neurite length nor diameter. These results indicate that Vps18–GFP delivery to neurites of polarized neuroendocrine cells is sensitive to acute perturbation of clathrin function.

DISCUSSION

Mouse mutants in subunits of HPS protein complexes and Vps33a, a Vps class C tether complex subunit, share phenotypes. The shared phenotypes suggests that associations between Vps33a and other HPS protein complexes participate in the same pathway, delivering membrane proteins from early endosomes to late endosomes/lysosomes and lysosome-related organelles (Suzuki *et al.*, 2003; Li *et al.*, 2004). Defects in this route trigger HPS in humans (Li *et al.*, 2004; Di Pietro and Dell'Angelica, 2005). Similarly, *S. cerevisiae* orthologues of

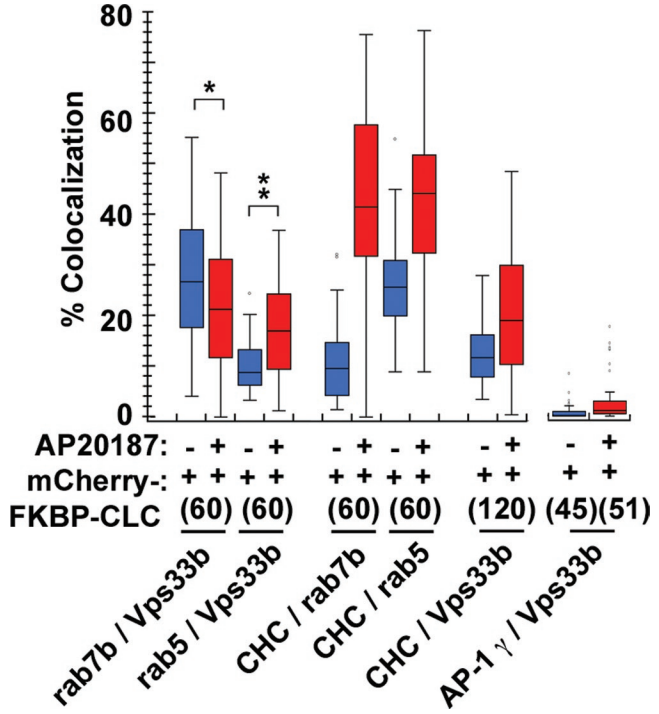

FIGURE 8: Chemical/genetic disruption of clathrin affects Vps33b distribution in Rab5 and Rab7b endosomal compartments. This figure depicts the quantification of experiments as those in Supplemental Figure 3. HEK293T cells expressing mCherry-FKBP–CLC (+) were treated in the presence of 0.05% vol/vol ethanol vehicle (−) or 50 nM AP20187 (+) for 2 h. Cells were triple stained with antibodies against CHC, Vps33b, and one of the following: rab5 or rab7b. Alternatively, cells were double labeled with AP-1 γ and Vps33b antibodies. Percentage of overlapping pixels between different antigen combinations was determined using Metamorph. Numbers depicted in parentheses denote number of analyzed images obtained from at least three independent experiments. * $p = 0.0288$, ** $p < 0.0001$, Wilcoxon–Mann–Whitney Rank Sum Test.

Vps class C proteins and AP-3 subunits participate in the delivery of cargoes to the vacuole. Genetic and/or biochemical interactions between AP-3 and HOPS subunits in yeast and vertebrates provide mechanistic insight into the molecular organization of this genetic pathway (Angers and Merz, 2009, 2010; Nickerson *et al.*, 2009; Salazar *et al.*, 2009). Our results are the first evidence of vertebrate Vps class C/HOPS proteins interacting with the early endosomal coats clathrin and AP-3 and the clathrin-binding scaffold Hrs. Moreover, we provide biochemical evidence of an interaction between Vps33a and AP-3 predicted from the phenotypic similarities between Vps33a- and AP-3-deficient mice. Clathrin and AP-3 highlight fundamental differences in the way that yeast and mammalian Vps class C and coats interact. In contrast with yeast AP-3, the mammalian ortholog of this adaptor complex interacts with clathrin (Seeger and Payne, 1992; Dell'Angelica *et al.*, 1998; Anand *et al.*, 2009). These observations suggest differences in the biochemical and functional architecture of mechanisms controlled by vertebrate Vps class C/HOPS–containing tethers and coats. Mammalian class C Vps proteins (Vps11, 16, 18, and 33a-b) and the HOPS-specific subunits Vps39 and Vps41 establish specific interactions with clathrin chains (Figure 2). We identified Vps class C/HOPS proteins in isolated clathrin-coated carriers, clathrin-positive domains of rab5-positive early endosomes, and rab7b-containing endosomes (Figures 3–5). The association of clathrin with Vps class C/HOPS proteins has at least two modalities: one occurring with the AP-3 complex and another in which Hrs participates. Clathrin–AP-3–Vps class C/HOPS and clathrin–Hrs–Vps class C/HOPS associations suggest vesicular and nonvesicular mechanisms controlling Vps class C/HOPS subunit subcellular distribution along the endocytic pathway, respectively.

We focused on the association between Vps class C/HOPS subunits and clathrin chains because quantitative fluorescence microscopy indicated a greater degree of overlap between Vps33b/Vps16 and CHC than with AP-3 (Figure 3J). The functionality of Vps class C/HOPS protein–clathrin interactions was demonstrated by acute perturbation of clathrin function (Moskowitz *et al.*, 2003; Deborde *et al.*, 2008). Chimeric CLC carrying the oligomerization module FKBP and AP20187 treatment rapidly redistributed CHC, class C Vps proteins (Vps18, Vps33b), and HOPS subunits (Vps39, Vps41) to organelles distributed throughout the cytoplasm and the perinuclear region (Figures 6–8). Quantitative immunofluorescence microscopy revealed that, upon clathrin function perturbation, Vps33b content preferentially increased in rab5-positive over either rab7b-containing endosomes or AP-1–positive organelles, such as the *trans*-Golgi (Figure 8 and Supplemental Figures 4 and 5). These findings support a model whereby clathrin-dependent mechanisms acutely define the subcellular distribution of Vps class C/HOPS-containing tethers. We directly tested this model in human cortical neurons and in NGF-differentiated PC12 cells, two polarized cellular models. We observed enrichment of class C Vps/HOPS subunits and clathrin at the tip of neurites (Figure 9A). Moreover, acute perturbation of clathrin function led to a progressive depletion of Vps18–GFP and mCherry-FKBP–CLC from the proximal segment of neurites imaged in vivo (Figure 9, B and C). We interpret this decrease in neurite Vps18–GFP and mCherry-FKBP–CLC fluorescence as the result of two concomitant processes: (1) inhibition of newly formed Vps18-clathrin–positive organelles entering the proximal neurite from the cell body plus (2) Vps18-clathrin–positive organelles already present in the neurite proximal segment at the time of drug addition progressively moving downstream toward the neurite tip.

Clathrin, AP-3, and Vps41 form a tripartite complex (Figure 2C). The association of Vps class C/HOPS subunits with clathrin, however, is independent of AP-3 expression levels (Figure 2D). Conversely, association of AP-3 and class C Vps/HOPS proteins is independent of clathrin expression (Figure 2E). These independent associations suggest that Vps class C/HOPS subunits establish multipronged interactions with clathrin and adaptors, such as AP-3 and/or that other clathrin-interacting molecules in early endosomes may mediate clathrin–Vps class C/HOPS subunit associations. We identified the early endosomal clathrin–Hrs flat coat participating in clathrin–Vps class C subunit interactions. Endogenous Hrs as well as recombinant Hrs coprecipitated endogenous clathrin and vps33b. Hrs and AP-3 mechanisms are likely independent because AP-3 is present in clathrin-coated vesicles yet Hrs is excluded from these coated carriers (Figure 5B). Therefore we propose that vesicular and nonvesicular clathrin–Vps class C/HOPS protein complexes regulate the subcellular distribution of class C Vps/HOPS subunits along the endocytic route. Structural predictions point to the presence of CHC homology domains in *S. cerevisiae* Vps 11, 18, 39, and 41, raising the possibility of multipronged associations between components of the coat and Vps class C/HOPS subunits (Darsow *et al.*, 2001; Nickerson *et al.*, 2009). Irrespective of whether multiple clathrin-binding molecules, such as AP-3 and Hrs, vesicular or nonvesicular mechanisms, or multipronged interactions between coats and Vps tethers exists, however, the redistribution of Vps class C/HOPS subunits upon of acute perturbation of clathrin function indicates that

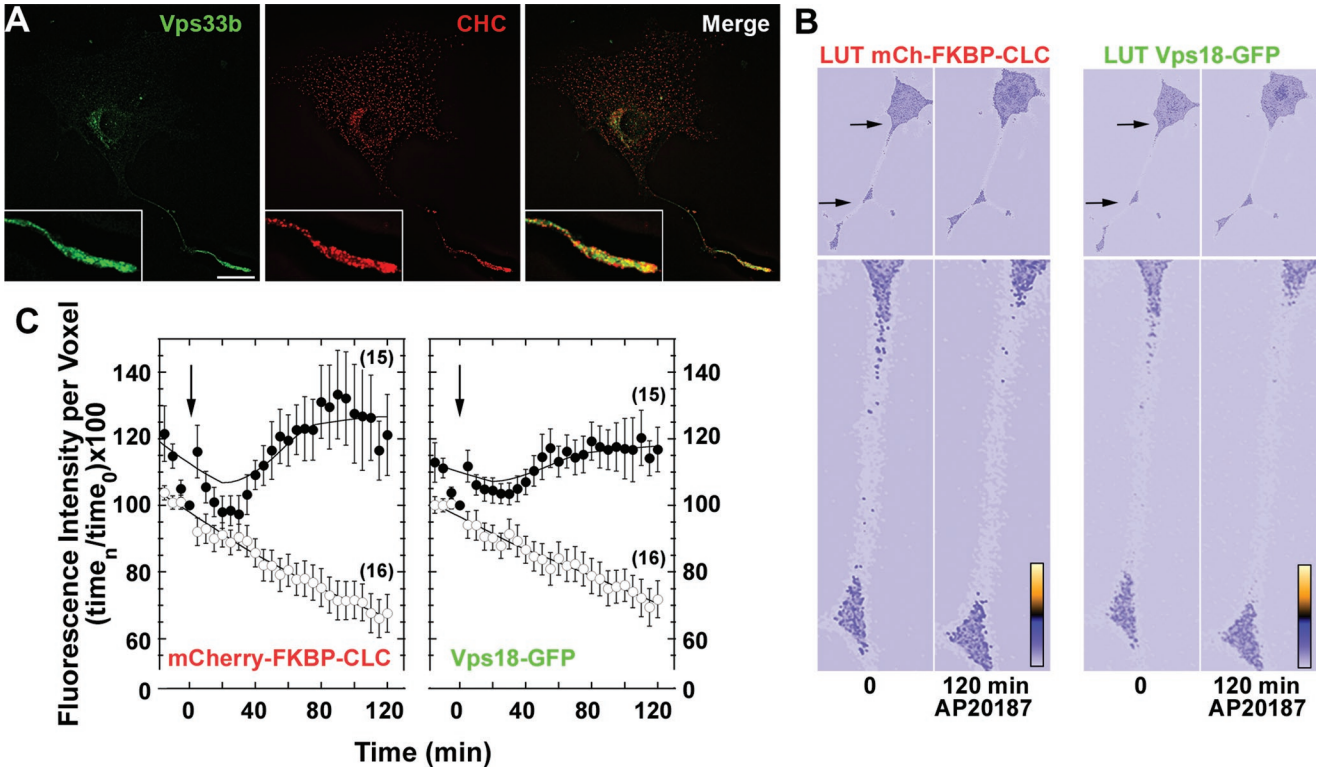

FIGURE 9: Polarized distribution of clathrin and Vps class C proteins in neuronal cells. (A) Human cortical neuronal cells, HCN-1, were fixed and processed for indirect immunofluorescence microscopy. Cells were double labeled with antibodies against endogenous Vps33b and CHC and imaged by high-resolution Delta deconvolution microscopy as previously described. HCN-1 cells that spontaneously extend processes in culture were imaged. (B) PC12 cells expressing recombinant mCherry-FKBP–CLC and Vps18–GFP were differentiated with NGF to induce process extension. Cells were imaged by live time-lapse confocal microscopy in the presence of 50 nM AP20187. Images of cells at time 0 and 120 min after drug addition are presented in (B). Panels depict images pseudocolored using the ICA LUT from Image J. Arrows mark the segment of the neurite where fluorescence intensities were measured over time. (C) Depicts a quantitative analysis of fluorescence intensity per voxel for mCherry-FKBP–CLC and Vps18–GFP. Neurite volume was measured in the proximal third of neurites as indicated by the arrows in (B). Closed circles correspond to cells imaged in the presence of ethanol vehicle (0.05% vol/vol), and open circles correspond to cells imaged in the presence of AP20187 (50 nM). Addition of either ethanol or AP20187 is marked by an arrow and corresponds to time 0. All data were normalized to the fluorescence intensity at time 0. Fluorescence intensities for mCherry-FKBP–CLC or Vps18–GFP at 60, 90, and 120 min after drug addition are significantly different from those from ethanol-treated cells ($p < 0.00015$, Wilcoxon–Mann–Whitney Rank Sum Test). Bar represents 20 μm.

significant pools of Vps class C/HOPS tethers are under control of clathrin-dependent mechanisms.

Angers and Merz have put forward an attractive model in which interactions between a tether, HOPS, and the coat AP-3 mediate docking of vesicles with the vacuole in *S. cerevisiae*, a process that culminates with fusion of membranes. Donor compartment (Golgi) and incoming AP-3–coated vesicles are devoid of HOPS complex in this model. HOPS complexes reside in the acceptor vacuolar compartments where coat and tether encounters occur to facilitate vesicle consumption (Angers and Merz, 2009, 2010). Our data suggest that, in addition to this mechanism, mammalian Vps class C/HOPS tethers are included in clathrin- and clathrin-AP-3–coated carriers, suggesting a coat-dependent mechanism for delivering Vps class C/HOPS tethers. Perturbing clathrin function with FKBP-CLC/AP20187 caused an increase in the number and size of organelles positive for Vps class C/HOPS subunits and trapped Vps33b in rab5-positive endosomes (Figures 6–8; Supplemental Figure 4). We attribute these effects to inhibition of clathrin-coated vesicle budding, consistent with published data (Moskowitz *et al.*, 2003; Deborde *et al.*, 2008) and possibly to changes in the dynamic of flat clathrin–Hrs coats in early endosomes. Alternatively, FKBP-CLC/AP20187 could possibly cause promiscuous recruitment of cytoplasmic Vps class C/HOPS protein pools to membranes by oligomerized FKBP–CLC. We do not favor this alternative hypothesis, however, because we do not detect an increased association of Vps33b to rab7b- or AP-1–positive organelles (Figure 8; Supplemental Figures 4 and 5).

AP-3 budding occurs mainly, if not exclusively, from transferrin receptor–positive endosomes (Peden *et al.*, 2004; Theos *et al.*, 2005; Craige *et al.*, 2008). Quantitative electron microscopy indicates that half of these AP-3 budding profiles possess clathrin on them (Peden *et al.*, 2004; Theos *et al.*, 2005). Perhaps, the presence of clathrin allows coats and Vps class C/HOPS subunits to be recruited at early stages in the vesicle life cycle. In the absence of clathrin, tethers and coats could undergo late interactions at target organelles, as proposed previously for yeast (Angers and Merz, 2009, 2010). Early inclusion of Vps class C/HOPS tethers into clathrin-coated carriers could serve a role for long-range delivery of tethers to polarized domains in mammalian cells. This hypothesis is supported by our findings that endogenous Vps33b and recombinantly expressed Vps18 and Vps39 display polarized distribution in the tip

of neurites in human cortical neurons or differentiated PC12 cells (Figure 9). An alternative yet nonexclusive model is that Vps class C/HOPS subunits could play a role in cargo selection either through indirect effects of Vps proteins on cargo recognition by coats or by direct association of class C Vps/HOPS proteins with SNAREs and nonSNARE membrane proteins. Support for this interpretation was obtained recently when *ema*/CLEC16A, which is a lectin-type membrane protein, was shown to directly bind to Vps16A in *Drosophila melanogaster* (Kim *et al.*, 2010).

At least four modalities of content delivery between stages of the endocytic route have been documented: vesicle-mediated (Stoorvogel *et al.*, 1996; Peden *et al.*, 2004), tubule-mediated transfer of cargoes (Delevoye *et al.*, 2009), kiss-and-run (Bright *et al.*, 2005), and endosome maturation (Stoorvogel *et al.*, 1991; Rink *et al.*, 2005; Poteryaev *et al.*, 2010). Endosome maturation is kinetically defined by the conversion over time of the same endosome membrane from a rab5- to a rab7-decorated compartment (Stoorvogel *et al.*, 1991; Rink *et al.*, 2005; Poteryaev *et al.*, 2010). This process depends on a switch mechanism in which a later acquisition of HOPS subunits promotes rab7 activation by interactors of the Vps39 subunit of HOPS (Nordmann *et al.*, 2010; Poteryaev *et al.*, 2010). Presently, it is unknown whether rab5 compartments can mature into rab7b compartments. We focused on rab7b because class C Vps/HOPS proteins were found in very low (background) levels in rab7- or LAMP-1–containing late endosomes (Figure 3J), suggesting that Vps class C/HOPS subunit binding may be short-lived on them. In contrast, class C Vps/HOPS associates to rab7b compartments. Rab7b has been implicated in delivery of Toll-like receptors from the cell surface to lysosomes in macrophages as well as in retrograde transport between endosomes and Golgi complex in HeLa cells (Wang *et al.*, 2007; Progida *et al.*, 2010). The presence of clathrin in rab7b-positive compartments and the observation that down-regulation of rab7b increases the expression level of AP-3 (Progida *et al.*, 2010) suggest a role of rab7b in vesicle-mediated transport between early endosomes and late endosomes/lysosomes or in a specialized retrograde transport between endosomes and the Golgi complex. Irrespective of whether rab7b-clathrin compartments represent vesicles, endosomes, or a combination thereof, our findings suggest that maturation of clathrin-coated membranes in transit among endosomal compartments could occur.

S. cerevisiae class C Vps proteins (Vps11, 16, 18, and 33) form a core that incorporates into CORVET and HOPS complexes (Peplowska *et al.*, 2007; Nickerson *et al.*, 2009; Ostrowicz *et al.*, 2010; Wickner, 2010). Vps8 and Vps3 constitute the CORVET complex whereas Vps39 and Vps41 establish specific interactions with the core defining the HOPS complex (Peplowska *et al.*, 2007; Markgraf *et al.*, 2009; Ostrowicz *et al.*, 2010). The organization and subcellular localization of HOPS has been partially characterized in metazoans (Kim *et al.*, 2001; Richardson *et al.*, 2004; Zhu *et al.*, 2009; Cullinane *et al.*, 2010). In contrast, metazoan CORVET has not been studied. Although putative human orthologues of CORVET subunits, Vps8/KIAA0804 and Vps3/TGFBRAP1, are present in databases, it remains unknown whether these gene products assemble with class C Vps proteins to form a mammalian CORVET complex. It is formally possible that mammalian class C Vps proteins, such as Vps33b and Vps16, identified in clathrin-containing organelles by biochemical and immunolocalization studies, may be part of both CORVET and HOPS complexes. The presence of class C vps subunits in both complexes might explain why there was a relatively higher colocalization between Vps33b/Vps16 (found in both CORVET and HOPS) and clathrin as compared with Vps41, Vps39, and clathrin (found only in HOPS; Figure 3). If this were the case, our data suggest that perturbing clathrin function affects Vps class C proteins along rab5 and rab7b compartments (Figure 8) by stalling maturation from a CORVET to a HOPS-positive-clathrin–coated vesicle or endosome.

Our results demonstrate a unique functional architecture of mechanisms controlled by vertebrate Vps class C/HOPS–containing tethers and clathrin coats. We postulate that clathrin-dependent mechanisms provide long-range and directional delivery of class C Vps/HOPS tethers to organelles and/or specialized domains of mammalian cells bearing complex architectures.

MATERIALS AND METHODS

Antibodies

The following antibodies were used in this study: polyclonal anti-myc (A190105A) and anti-HA (A190108A; Bethyl Laboratories, Montgomery, TX); polyclonal anti-GFP (cat# GFP-1020, Aves Labs, Tigard, OR, and cat# 132002, Synaptic Systems, Gottingen, Germany); monoclonal anti–Lamp H4A3, anti-SV2, and anti-AP3δ SA4 (Developmental Studies Hybridoma Bank, Iowa City, IA); monoclonal anti–rab7 ab50533 (Abcam, Cambridge, MA); monoclonal anti–rab7b clone 3B3 (Abnova, Taipei, Taiwan); monoclonal anti-rab5, anti–AP1γ adaptin, anti–rabaptin 5, and anti-EEA1 (610724, A36120, 610676, and 610456; BD Bioscience Transduction Laboratories, Pasadena, CA); monoclonal anti–CHC X22 (Calbiochem, San Diego, CA); monoclonal anti–CLC CON.1 (MMS423P; Covance, Berkeley, CA); polyclonal anti–mCherry dsRed (632496; Clontech, Mountain View, CA); monoclonal anti-AP2α adaptin and anti-actin (A4325 and A5441; Sigma, St. Louis, MO); polyclonal anti-AP3β1 (13384–1-AP; ProteinTech Group, Chicago, IL); monoclonal anti–GFP 3E6 (A11120; Molecular Probes, Eugene, OR); monoclonal anti–HRS A-5 (Enzo Life Sciences, Plymouth Meeting, PA); anti–synaptophysin clone SY38 (Millipore, Billerica, MA); and monoclonal anti–transferrin receptor H68.4 (136800; Zymed Laboratories, San Francisco, CA). Anti-Vps33b, anti-Spe39, and anti–AP3 β3 have been previously described (Faundez and Kelly, 2000; Salazar *et al.*, 2009; Zhu *et al.*, 2009). Anti-VAMP7 was a gift from Andrew Peden (Department of Clinical Biochemistry, University of Cambridge, UK). Immunofluorescence secondary antibodies were Alexa Fluor 488, 555, 568, or 647 anti–rabbit, rat, chicken, or isotype specific mouse IgG (Molecular Probes). The secondary antibodies used on Western blots were horseradish peroxidase-goat anti-mouse or anti-rabbit (626420 and G21234; Invitrogen, Carlsbad, CA).

Plasmids, oligos, and peptides

Plasmids encoding C-terminally tagged murine Vps11–HA and Vps16–HA, and N-terminally tagged GFP-murine Vps18 and GFP–Vps39 were gifts from Robert Piper (Department of Molecular Physiology and Biophysics, University of Iowa, Iowa City, IA), Vps18–myc from Liping Wang (Human Nutrition Research Center, UC Davis, CA), N-terminally tagged myc–HRS from Harold Stenmark (Institute for Cancer Research; Oslo University Hospital) (Raiborg *et al.*, 2002), and N-terminally tagged GFP–Rab5Q79L from Laura Volpicelli (University of Pennsylvania) (Volpicelli *et al.*, 2001). Spe39-enhanced GFP and HA-tagged Vps33a and Vps33b have been described (Zhu *et al.*, 2009).

C-terminal Vps41–myc was created from human Vps41 cDNA clone (cat# SC111791; Origene, Rockville, MD) and the primers 5′ caccatggcggaagcagaggag and 3′ ttggagatgaaaaaagaacaaaaacttatttctgaagaagatctgtag using PCR. The PCR product was cloned into

TOPO vector pcDNA 3.1 (Invitrogen), following the manufacturer's directions. The TOPO vector DNA was subsequently cut with enzymes *Bam*HI and *Eco*RV, and the Vps41–myc fragment was subcloned into pIREShyg3. The resulting clone was confirmed as error-free by DNA sequencing.

An N-terminally tagged HA–FKBP–CLC construct was the gift of Enrique Rodriguez-Boulan (Deborde *et al.*, 2008). This construct was modified by replacing the HA tag with a fluorescent mCherry tag as follows. We designed PCR primers complementary to mCherry that were flanked by *Nhe*I 5′ and *Bgl*II 3′(5′ GCTAGCATGGTGAGCAAGGGC and 3′ AGATCTCTTGTACAGCTCGTCCATGC) sites to allow cloning from a pmCherry vector (Clontech) into the TOPO TA 2.1 vector (Invitrogen). The TOPO TA 2.1 mCherry vector and the HA-FKBP–CLC PCR product were each digested with *Nhe*I and *Bgl*II. Appropriately sized DNA bands were identified on an agarose gel, extracted, and ligated to create mCherry-FKBP–CLC. Coding sequence was verified as error-free by DNA sequencing. The ARGENT Regulated Homodimerization Kit containing FKBP plasmids and the dimerization drug AP20187 was purchased from ARIAD (www.ariad.com; Cambridge; MA).

All siRNA oligos were purchased from Dharmacon (Lafayette, CO). The siCONTROL Non-Targeting siRNA Pool #1 (D0012061305) was used for control knockdown. siGENOME human CLTC, NM_004859 siRNA was used for CHC knockdown (D00400102) sense: GCAAUGAGCUGUUUGAAGAUU, antisense: 5′ pUCUUCAAACAGCUCAUUGCUU. siRNA oligos were transfected as described later in the text. AP3δ (RHS4533-NM_003938) and CHC (RHS39799577067) shRNA in a pLKO.1 vector for lentiviral infection were obtained from Open Biosystems (Huntsville, AL). Control shRNA in pLKO.1 was obtained from Addgene (vector 1864; Cambridge, MA).

The peptide against the epitope for AP3δ SA4 (AQQVDIVTEEMPENALPSDEDDKDPNDPYRA) (Salazar *et al.*, 2009) was purchased from the Emory Microchemical Facility (Atlanta, GA) and Invitrogen (EvoQuest Team, Carlsbad, CA).

Cell culture, transfection, and lenti viral infection

HEK293T and HCN-1A cells (American Type Culture Collection [ATCC], Manassas, VA) in DMEM (Hyclone, Logan, UT) supplemented with 10% fetal bovine serum (FBS) (Hyclone) and 100 µg/ml penicillin and streptomycin (Hyclone) and PC12 cells (ATCC) in DMEM supplemented with 5% FBS, 10% equine serum (Hyclone), and 100 µg/ml penicillin and streptomycin (Hyclone) were incubated at 37°C with 10% CO_2.

For recombinant DNA expression, HEK293T cells were transfected in six-well dishes with 0.5–2.0 µg DNA in 0.25% Lipofectamine 2000 (Invitrogen) diluted in Opti-Mem (Life Technologies, Grand Island, NY). Cells were transfected for 4 h followed by incubation in either culture medium alone or culture medium containing the selection drug(s) G418 (0.1 mg/ml) and/or hygromycin (0.1 mg/ml) for the maintenance of stable cell lines. PC12 cells were transfected by nucleofection with 3 µg of DNA using Amaxa Cell Line Nucleofector Kit V (cat# VCA-1003; Lonza Walkersville, Koeln, Germany, www.lonza.com), and were plated on Matrigel-coated glass-bottom culture dishes (Matek, Ashland, MA) in PC12 culture medium supplemented with 100 ng/ml NGF 2.5S (murine, natural) (cat# 13257-019; Invitrogen). PC12 cells were differentiated for 48–72 h at 37°C with 10% CO_2 For siRNA knockdown, HEK293T cells were transfected in six-well dishes with 50 nM oligo for 4 h, incubated for 20 h in culture medium, and transfected a second time with 50 nM oligo for 4 h followed by incubation for 3 d in culture medium. For lentiviral infection, HEK293T cells seeded in 10-cm plates were infected with 1 µl of high-titer lentivirus containing the shRNA constructs mentioned earlier in the text. Following a 24-h infection, cells were incubated for up to 6 d in culture medium supplemented with 4 µg/ml puromycin for selection. The Emory Neuroscience NINDS Viral Vector Core Facilities prepared all high-titer lentiviruses.

Cross-linking and immunoprecipitation

Cross-linking was performed as previously described using DSP (Craige *et al.*, 2008; Salazar *et al.*, 2009; Zlatic *et al.*, 2010). DSP is a homobifunctional reversible and cell-permeable cross-linker with a 12-Å spacer arm that stabilizes labile protein interactions (Lomant and Fairbanks, 1976). Plates of confluent HEK293T cells were placed on ice, washed twice with ice-cold phosphate-buffered saline (PBS)/1 mM $MgCl_2$/0.1 mM $CaCl_2$, and then incubated with 1 mM DSP (cat# 22585; Thermo Scientific, Rockford, IL) or dimethyl sulfoxide control in PBS/1 mM $MgCl_2$/0.1 mM $CaCl_2$ for 2 h on ice. DSP was then quenched with 25 mM TRIS, pH 7.4, followed by two rinses with ice-cold PBS/1 mM $MgCl_2$/0.1 mM $CaCl_2$. Cells were lysed in Buffer A (150 mM NaCl, 10 mM HEPES, 1 mM EGTA, 0.1 mM $MgCl_2$) + 0.5% Triton X-100 by incubation for 30 min at 4°C. Any remaining cellular debris was scraped from plates and centrifuged at 16,000 × *g* for 10 min. The supernatant was collected, diluted to 1 µg/ul in Buffer A + 0.5% Triton X-100, and incubated with Dynal immunomagnetic precipitation beads (Dynal, Oslo, Norway) in the absence or presence of a 10 µM SA4 peptide competitor. Beads and lysate were incubated at 4°C for 2 h and washed six times with Buffer A containing 0.1% Triton X-100 to remove nonspecifically bound material. The material that remained bound after these washes was then eluted by treatment with either the peptide antigen or SDS–PAGE sample buffer followed by incubation at 75°C for 5 min. Immunoprecipitated material was analyzed on SDS–PAGE Western blot.

Despite reduced detection of δ in SA4 immunoprecipitates, all other AP-3 subunits are readily detectable in these immunocomplexes (Salazar *et al.*, 2009). Decreased detection of AP-3 δ by the SA4 mAb in immunoblots after DSP cross-linking likely reflects a chemical modification of the SA4 epitope by the cross-linking agent. The lysine and arginine present in this peptide are susceptible to modification by DSP. The SA4 antibody is used sequentially in immunoprecipitation and immunoblot, thus effectively magnifying the difference between (–) and (+) DSP samples.

Immunolocalization, microscopy, and quantification

Coverslips were prepared as previously described (Faundez *et al.*, 1997). Cells were seeded onto Matrigel (BD Bioscience, San Jose, CA)-coated glass coverslips, washed twice in PBS/1 mM $MgCl_2$/0.1 mM $CaCl_2$, and fixed using 4% paraformaldehyde in PBS. Cells were then permeabilized and blocked with 0.02% saponin (Sigma), 15% horse serum (Hyclone), 2% bovine serum albumin, and 1% fish skin gelatin (Sigma) in PBS. Blocked and permeabilized cells were incubated with the primary and secondary antibodies described earlier in the text and were mounted with Gelvatol onto slides. Fixed-cell confocal microscopy was performed on fixed cells as described (Deborde *et al.*, 2008) using an Axiovert 100M microscope (Carl Zeiss, Thornwood, NY) with Argon/HeNe (488/543) laser excitation. Images were captured using a Plan Apochromat 63×/1.4 oil DIC objective, BP 505–550/LP 560 filter set, and LSM 510 3.2.0.104 software (Carl Zeiss). Deconvolution microscopy was performed as described (Deborde *et al.*, 2008) with a 200M inverted microscope using 63×/1.4 and 100×/1.4 oil DIC objectives (Carl Zeiss) and a Sedat filter set. Images were collected using a

scientific grade cooled charge-coupled Cool-Snap HQ camera with ORCA-ER chip on a multiwavelength, wide-field, three-dimensional microscopy system using Slidebook 4.0 OS X software (Intelligent Imaging Innovations, Denver, CO). Out-of-focus light was removed with a constrained iterative deconvolution algorithm (Swedlow *et al.*, 1997). Confocal and deconvolution images were processed and analyzed using LSM Image Browser 4.0.0.157 (Carl Zeiss), Metamorph software version 6.1 (Universal Imaging, Sunnyvale, CA), and Imaris 6.3.1 software (Bitplane, St. Paul, MN). Colocalization and puncta size were determined from three consecutive z-series focal planes per image. All channels were thresholded individually. Percent colocalization was determined by calculation of pixel area containing fluorescent signals from two channels per total pixel area for a single fluorophore. Puncta size was determined by integrated morphometric analysis of total pixel area within puncta as determined by image thresholding.

Clathrin-coated vesicle isolation

HEK293T or HEK293T cells stably expressing tagged HOPS or class C Vps proteins were used to prepare clathrin-coated vesicles as described previously (alternate protocol 2 in Girard *et al.*, 2004). Briefly, cells were grown to confluence and washed twice with PBS/1 mM $MgCl_2$/0.1 mM $CaCl_2$. Cells were lifted in CCV buffer (100 mM MES, 1.0 mM EGTA, 0.5 mM $MgCl_2$, pH 6.5), transferred to a Potter Elvehjem glass-teflon homogenizer, and homogenized for 10 strokes at 1500 rpm on a Tri-R Stir-R variable speed laboratory motor (Model S63C; Tri-R Instruments, Rockville Center, NY). Homogenate was centrifuged in an SS-34 fixed-angle rotor for 20 min at 17,000 × *g*, 4°C. The resulting supernatant was further centrifuged in a type 40 fixed-angle rotor for 60 min at 56,000 × *g*, 4°C. The resulting pellet was resuspended, homogenized, and transferred to polyallomer centrifuge tubes (Beckman, Palo Alto, CA). The sample was then underlaid with D_2O-sucrose solution (8% sucrose, 100 mM MES, 1.0 mM EGTA, 0.5 mM $MgCl_2$, D_2O) (D_2O cat# 364312-10G; Sigma) and was centrifuged in a SW-55 swing-bucket rotor for 2 h at 116,000 × *g*, 4°C. This final, clathrin-coated, vesicle-enriched pellet was resuspended and aliquoted along with reserves from previous fractionation steps and was run on SDS–PAGE gels for Western blotting or Coomassie stain.

Acute clathrin perturbation

HEK293T or HEK293T cells stably expressing tagged HOPS or class C Vps proteins and/or transiently expressing tagged FKBP–CLC were incubated for 2 h at 37°C, 10% CO_2 in culture medium supplemented with 50 nM AP20187 (ARIAD) or 0.05% ethanol vehicle control. Culture dishes were then placed on ice and processed for either immunolocalization or cross-linking followed by immunoprecipitation.

Live cell imaging

HEK293T or PC12 cells expressing Vps18–GFP and/or mCherry-FKBP–CLC were grown on Matrigel-coated glass-bottom culture dishes (Matek). Imaging medium consisted of Hank's balanced salt solution minus phenol red and $NaHCO_2$ (Sigma) and supplemented with 10% FBS (Hyclone) and 20 mM HEPES for HEK293T, and with 10% Donor Equine Serum (Hyclone), 5% FBS (Hyclone), and 100 ng/ml NGF 2.5S (murine, natural, cat# 13257–019; Invitrogen) for PC12 cells. Live imaging was performed on an A1R Laser Scanning Confocal Microscope (Nikon, Melville, NY) equipped with a hybrid scanner, Perfect Focus, and an environmental chamber for regulation of temperature to 37°C and 10% CO_2. Fluorophores were alternately excited with 488 and 568 nm wavelength laser every 5 min for 2 h and 30 min. AP20187 (Ariad) or ethanol vehicle control was added to imaging medium at concentrations listed earlier in the text after the first 25 min of imaging. Images were captured with an APO TIRF 60×/1.49 oil DIC objective and 500–550/570–620 filter sets on NIS-Elements AR 3.1 (Nikon) software. NIS-Elements AR 3.0, Imaris 6.3.1 (Bitplane), and Image J 1.41(NIH) software were used for image analysis.

Statistical analysis

Experimental conditions were compared with the nonparametric Wilcoxon–Mann–Whitney Rank Sum Test using Synergy KaleidaGraph v4.03 (Reading, PA) or StatPlus Mac Built5.6.0pre/Universal (AnalystSoft, Vancouver, Canada). Data are presented as boxplots displaying the four quartiles of the data, with the "box" comprising the two middle quartiles, separated by the median. The upper and lower quartiles are represented by single lines extending from the box. Circles correspond to outlier points defined by the statistical software as beyond the upper or lower quartile plus 1.5 times the value of the 2–3 interquartile distance.

ACKNOWLEDGMENTS

This work was supported by grants from the National Institutes of Health to V.F. (NS42599 and GM077569) and to S.W.L. (GM082932) and by the University Research Committee. S.A.Z. was supported by T32 GM008367, National Institutes of Health, Training Program in Biochemistry, Cell, and Molecular Biology. We are indebted to the Faundez lab members for their comments. The work was also supported by the Neuronal Imaging and Lentiviral Cores of the Emory Neuroscience NINDS Core Facilities Grant P30NS055077.

REFERENCES

Anand VC, Daboussi L, Lorenz TC, Payne GS (2009). Genome-wide analysis of AP-3-dependent protein transport in yeast. Mol Biol Cell 20, 1592–1604.

Angers CG, Merz AJ (2009). HOPS interacts with Apl5 at the vacuole membrane and is required for consumption of AP-3 transport vesicles. Mol Biol Cell 20, 4563–4574.

Angers CG, Merz AJ (2011). New links between vesicle coats and Rab-mediated vesicle targeting. Semin Cell Dev Biol 22, 18–26.

Bonifacino JS, Glick BS (2004). The mechanisms of vesicle budding and fusion. Cell 116, 153–166.

Borner GH, Harbour M, Hester S, Lilley KS, Robinson MS (2006). Comparative proteomics of clathrin-coated vesicles. J Cell Biol 175, 571–578.

Bright NA, Gratian MJ, Luzio JP (2005). Endocytic delivery to lysosomes mediated by concurrent fusion and kissing events in living cells. Curr Biol 15, 360–365.

Craige B, Salazar G, Faundez V (2008). Phosphatidylinositol-4-kinase type II alpha contains an AP-3 sorting motif and a kinase domain that are both required for endosome traffic. Mol Biol Cell 19, 1415–1426.

Cullinane AR *et al.* (2010). Mutations in VIPAR cause an arthrogryposis, renal dysfunction and cholestasis syndrome phenotype with defects in epithelial polarization. Nat Genet 42, 303–312.

Darsow T, Katzmann DJ, Cowles CR, Emr SD (2001). Vps41p function in the alkaline phosphatase pathway requires homo-oligomerization and interaction with AP-3 through two distinct domains. Mol Biol Cell 12, 37–51.

Deborde S, Perret E, Gravotta D, Deora A, Salvarezza S, Schreiner R, Rodriguez-Boulan E (2008). Clathrin is a key regulator of basolateral polarity. Nature 452, 719–723.

Delevoye C *et al.* (2009). AP-1 and KIF13A coordinate endosomal sorting and positioning during melanosome biogenesis. J Cell Biol 187, 247–264.

Dell'Angelica EC (2009). AP-3-dependent trafficking and disease: the first decade. Curr Opin Cell Biol 21, 552–559.

Dell'Angelica EC, Klumperman J, Stoorvogel W, Bonifacino JS (1998). Association of the AP-3 adaptor complex with clathrin. Science 280, 431–434.

Di Pietro SM, Dell'Angelica EC (2005). The cell biology of Hermansky-Pudlak syndrome: recent advances. Traffic 6, 525–533.
Faundez V, Horng JT, Kelly RB (1997). ADP ribosylation factor 1 is required for synaptic vesicle budding in PC12 cells. J Cell Biol 138, 505–515.
Faundez V, Kelly RB (2000). The AP-3 complex required for endosomal synaptic vesicle biogenesis is associated with a casein kinase I alpha-like isoform. Mol Biol Cell 11, 2591–2604.
Girard M, Allaire PD, Blondeau F, McPherson PS (2004). Isolation of clathrin-coated vesicles. In: Current Protocols in Cell Biology, vol. 1, ed. JS Bonifacino, M Dasso, J Harford, J Lippincott-Schwartz, and K. Yamada, New York: John Wiley & Sons, 3.13.11–13.13.31.
Kim BY, Kramer H, Yamamoto A, Kominami E, Kohsaka S, Akazawa C (2001). Molecular characterization of mammalian homologues of class C Vps proteins that interact with syntaxin-7. J Biol Chem 276, 29393–29402.
Kim S, Wairkar YP, Daniels RW, DiAntonio A (2010). The novel endosomal membrane protein Ema interacts with the class C Vps-HOPS complex to promote endosomal maturation. J Cell Biol 188, 717–734.
Li W, Rusiniak ME, Chintala S, Gautam R, Novak EK, Swank RT (2004). Murine Hermansky-Pudlak syndrome genes: regulators of lysosome-related organelles. Bioessays 26, 616–628.
Lomant AJ, Fairbanks G (1976). Chemical probes of extended biological structures: synthesis and properties of the cleavable protein cross-linking reagent [35S]dithiobis(succinimidyl propionate). J Mol Biol 104, 243–261.
Markgraf DF, Ahnert F, Arlt H, Mari M, Peplowska K, Epp N, Griffith J, Reggiori F, Ungermann C (2009). The CORVET subunit Vps8 cooperates with the Rab5 homolog Vps21 to induce clustering of late endosomal compartments. Mol Biol Cell 20, 5276–5289.
Moskowitz HS, Heuser J, McGraw TE, Ryan TA (2003). Targeted chemical disruption of clathrin function in living cells. Mol Biol Cell 14, 4437–4447.
Nickerson DP, Brett CL, Merz AJ (2009). Vps-C complexes: gatekeepers of endolysosomal traffic. Curr Opin Cell Biol 21, 543–551.
Nordmann M, Cabrera M, Perz A, Brocker C, Ostrowicz C, Engelbrecht-Vandre S, Ungermann C (2010). The Mon1-Ccz1 complex is the GEF of the late endosomal Rab7 homolog Ypt7. Curr Biol 20, 1654–1659.
Odorizzi G, Cowles CR, Emr SD (1998). The AP-3 complex: a coat of many colours. Trends Cell Biol 8, 282–288.
Ostrowicz CW, Brocker C, Ahnert F, Nordmann M, Lachmann J, Peplowska K, Perz A, Auffarth K, Engelbrecht-Vandre S, Ungermann C (2010). Defined subunit arrangement and Rab interactions are required for functionality of the HOPS tethering complex. Traffic 11, 1334–1346.
Ostrowicz CW, Meiringer CT, Ungermann C (2008). Yeast vacuole fusion: a model system for eukaryotic endomembrane dynamics. Autophagy 4, 5–19.
Peden AA, Oorschot V, Hesser BA, Austin CD, Scheller RH, Klumperman J (2004). Localization of the AP-3 adaptor complex defines a novel endosomal exit site for lysosomal membrane proteins. J Cell Biol 164, 1065–1076.
Peplowska K, Markgraf DF, Ostrowicz CW, Bange G, Ungermann C (2007). The CORVET tethering complex interacts with the yeast Rab5 homolog Vps21 and is involved in endo-lysosomal biogenesis. Dev Cell 12, 739–750.
Poteryaev D, Datta S, Ackema K, Zerial M, Spang A (2010). Identification of the switch in early-to-late endosome transition. Cell 141, 497–508.
Progida C, Cogli L, Piro F, De Luca A, Bakke O, Bucci C (2010). Rab7b controls trafficking from endosomes to the TGN. J Cell Sci 123, 1480–1491.
Raiborg C, Bache KG, Gillooly DJ, Madshus IH, Stang E, Stenmark H (2002). Hrs sorts ubiquitinated proteins into clathrin-coated microdomains of early endosomes. Nat Cell Biol 4, 394–398.
Raiborg C, Wesche J, Malerod L, Stenmark H (2006). Flat clathrin coats on endosomes mediate degradative protein sorting by scaffolding Hrs in dynamic microdomains. J Cell Sci 119, 2414–2424.
Rehling P, Darsow T, Katzmann DJ, Emr SD (1999). Formation of AP-3 transport intermediates requires Vps41 function. Nat Cell Biol 1, 346–353.
Richardson SC, Winistorfer SC, Poupon V, Luzio JP, Piper RC (2004). Mammalian late vacuole protein sorting orthologues participate in early endosomal fusion and interact with the cytoskeleton. Mol Biol Cell 15, 1197–1210.
Rink J, Ghigo E, Kalaidzidis Y, Zerial M (2005). Rab conversion as a mechanism of progression from early to late endosomes. Cell 122, 735–749.
Ronnett GV, Hester LD, Nye JS, Connors K, Snyder SH (1990). Human cortical neuronal cell line: establishment from a patient with unilateral megalencephaly. Science 248, 603–605.
Salazar G, Craige B, Wainer BH, Guo J, De Camilli P, Faundez V (2005). Phosphatidylinositol-4-kinase type II {alpha} is a component of adaptor protein-3-derived vesicles. Mol Biol Cell 16, 3692–3704.
Salazar G, Zlatic S, Craige B, Peden AA, Pohl J, Faundez V (2009). Hermansky-Pudlak syndrome protein complexes associate with phosphatidylinositol 4-kinase type II alpha in neuronal and nonneuronal cells. J Biol Chem 284, 1790–1802.
Seeger M, Payne GS (1992). A role for clathrin in the sorting of vacuolar proteins in the Golgi complex of yeast. EMBO J 11, 2811–2818.
Stoorvogel W, Oorschot V, Geuze HJ (1996). A novel class of clathrin-coated vesicles budding from endosomes. J Cell Biol 132, 21–33.
Stoorvogel W, Strous GJ, Geuze HJ, Oorschot V, Schwartz AL (1991). Late endosomes derive from early endosomes by maturation. Cell 65, 417–427.
Suzuki T, Oiso N, Gautam R, Novak EK, Panthier JJ, Suprabha PG, Vida T, Swank RT, Spritz RA (2003). The mouse organellar biogenesis mutant buff results from a mutation in Vps33a, a homologue of yeast vps33 and Drosophila carnation. Proc Natl Acad Sci USA 100, 1146–1150.
Swedlow JR, Sedat JW, Agard DA (1997). Deconvolution in optical microscopy. In: Deconvolution of Images and Spectra, ed. PA Jansson, San Diego, CA: Academic Press, 284–307.
Theos AC *et al.* (2005). Functions of adaptor protein (AP)-3 and AP-1 in tyrosinase sorting from endosomes to melanosomes. Mol Biol Cell 16, 5356–5372.
Volpicelli LA, Lah JJ, Levey AI (2001). Rab5-dependent trafficking of the m4 muscarinic acetylcholine receptor to the plasma membrane, early endosomes, and multivesicular bodies. J Biol Chem 276, 47590–47598.
Wang Y, Chen T, Han C, He D, Liu H, An H, Cai Z, Cao X (2007). Lysosome-associated small Rab GTPase Rab7b negatively regulates TLR4 signaling in macrophages by promoting lysosomal degradation of TLR4. Blood 110, 962–971.
Wickner W (2010). Membrane fusion: Five lipids, four SNAREs, three chaperones, two nucleotides, and a Rab, all dancing in a ring on yeast vacuoles. Annu Rev Cell Dev Biol 26, 115–136.
Zhu GD, Salazar G, Zlatic SA, Fiza B, Doucette MM, Heilman CJ, Levey AI, Faundez V, L'Hernault S W (2009). SPE-39 family proteins interact with the HOPS complex and function in lysosomal delivery. Mol Biol Cell 20, 1223–1240.
Zlatic SA, Ryder PV, Salazar G, Faundez V (2010). Isolation of labile multi-protein complexes by in vivo controlled cellular cross-linking and immuno-magnetic affinity chromatography. J Vis Exp 1855 [pii] 1810.3791/1855.